

Evaluation of lower quality recycled PCCP for Portland cement treated base (PCTB)

by

Koby Francis Daily

B.S., Kansas State University, 2016

A THESIS

submitted in partial fulfillment of the requirements for the degree

MASTER OF SCIENCE

Department of Civil Engineering  
College of Engineering

KANSAS STATE UNIVERSITY  
Manhattan, Kansas

2018

Approved by:

Major Professor  
Dr. Christopher Jones

# **Copyright**

© Koby Daily 2018.

## **Abstract**

With recycled concrete aggregates (RCA) becoming a more popular and cost effective alternative to virgin aggregate, the Kansas Department of Transportation (KDOT) looks to incorporate these aggregates into Portland cement treated base (PCTB). KDOT currently practices a freeze-thaw method that includes 90 days of curing and a maximum of 660 freeze-thaw cycles to determine the durability of its concrete pavements and bases. An experimental study was conducted to determine if lower quality RCA would be an adequate replacement for virgin aggregates within PCTB. Two sources of D-cracked aggregate from “D” cracked pavements, were acquired and used to batch the PCTB. Control samples were batched using virgin aggregates following the gradation of the two sources of RCA. Following the procedure laid out by KDOT, both the RCA and control samples were tested for durability. The results showed that increasing the total amount of cementitious binder in the PCTB increased the durability. Also at lower binder contents, the type of RCA had an impact on the performance of the base containing RCA. In addition, the RCA and control samples had similar performance, and as a result RCA could be a viable aggregate source for PCTB. Finally, it was determined that different criteria need to be developed for the freeze-thaw durability of PCTB as mass loss was an important factor for PCTB with D-cracked aggregates.

## Table of Contents

List of Figures .....	vii
List of Tables .....	ix
Acknowledgements .....	x
Chapter 1 - Introduction .....	1
1.1 Background .....	1
1.2 Problem Statement .....	1
1.3 Objectives .....	2
1.4 Study Method .....	2
1.5 Thesis Outline .....	2
Chapter 2 - Literature Review .....	4
2.1 Recycled Concrete Aggregates (RCA) .....	4
2.1.1 <i>Physical Properties of RCA</i> .....	4
2.1.2 <i>RCA Production</i> .....	5
2.2 D-Cracking of Coarse Aggregate .....	5
2.2.1 <i>Mechanism of D-Cracking</i> .....	5
2.2.2 <i>Appearance and Progression of D-Cracking</i> .....	6
2.2.3 <i>Conditions for D-Cracking</i> .....	6
2.2.4 <i>Non-influential Factors</i> .....	7
2.2.5 <i>Prevention</i> .....	7
2.3 Freeze-Thaw Resistance of Concrete .....	7
2.3.1: <i>Mechanisms of Internal Damage</i> .....	8
2.3.2: <i>Effects of Surface Scaling</i> .....	9
2.3.4: <i>Effect of Drying</i> .....	9
2.4 Durable Aggregate and Concrete Identification Procedures .....	10
2.4.1 <i>KTMR-21: Soundness &amp; Modified Soundness of Aggregates by Freezing and Thawing</i> .....	10
2.4.2 <i>ASTM C666: Rapid Freezing and Thawing of Concrete</i> .....	10
2.4.3 <i>ASTM C88: Aggregate Sulfate Soundness</i> .....	11
2.4.4 <i>ASTM C295 Petrographic Examination of Aggregates for Concrete</i> .....	12
2.4.5 <i>Washington Hydraulic Fracture Test</i> .....	12

2.5 Curing Methods for Freeze-Thaw Testing.....	12
2.5.1 Microwave and Steam Curing .....	13
2.5.2 Temperature-Match-Curing.....	13
2.6 Modified Versions of ASTM C666 .....	14
2.6.1 Kansas Department of Transportation .....	14
2.6.2 Other Organization's Methods .....	15
2.7 Summary.....	15
Chapter 3 - Materials .....	17
3.1 Coarse Aggregate.....	17
3.2 Fine Aggregate.....	18
3.3 Cement .....	19
3.4 Fly Ash.....	20
Chapter 4 - Methods.....	21
4.1 PCTB Mix Design .....	21
4.2 Moisture-Density Curve .....	21
4.3 Compression Testing .....	22
4.4 Cement Treated Base Batching.....	24
4.5 Preparation of Cement Treated Base Prisms .....	25
4.6 ASTM C666 Testing.....	25
4.6.1 Mass Measurements.....	26
4.6.2 Resonant Frequency Measurements .....	26
4.6.3 Expansion Measurements .....	29
Chapter 5 - D-Cracked RCA Cement Treated Base Study Results .....	30
5.1 Change in Mass.....	30
5.2 Relative Dynamic Modulus of Elasticity .....	30
5.3 Expansion.....	31
Chapter 6 - Control Portland Cement Treated Base Results.....	33
6.1 Change in Mass.....	36
6.2 Relative Dynamic Modulus of Elasticity .....	36
6.3 Expansion.....	37
Chapter 7 - Analysis and Discussion .....	38

7.1 D-Cracked RCA Cement Treated Base .....	38
7.2 Control Portland Cement Treated Base .....	40
Chapter 8 - Conclusions.....	42
8.1 Recommendations for Future Research.....	42
References.....	43
Appendix A - D-Cracked RCA Moisture Density Curves.....	46
Appendix B - D-Cracked RCA ASTM C666 Results .....	47
Appendix C - Control Moisture Density Curves .....	51
Appendix D - Control ASTM C666 Results.....	53
Appendix E - Comparison of PCTB with RCA to Control .....	55

## List of Figures

Figure 4.1 KC 100% Cement Moisture Density Curve .....	22
Figure 4.2 KDOT Example PCTB Blend .....	23
Figure 4.3 James E-Meter™ Mk II with Accelerometer and Impactor.....	26
Figure 4.4 Transverse Frequency Wave of Sample before Testing.....	27
Figure 4.5 Transverse Frequency Wave of Sample Near Failure.....	28
Figure 4.6 Typical Sample Transverse Frequency .....	28
Figure 6.1: Topeka Control Blend Curve .....	33
Figure 6.2: KC Control Blend Curve.....	34
Figure 7.1 Average RCA RDME Trend During Study.....	38
Figure 7.2 RCA Mass Change During Study.....	39
Figure 7.3 Control Sample RDME Trend During Study .....	41
Figure 7.4 KC RCA and Control RDME Trend Comparison.....	41
Figure A.1 Topeka 100% Cement Moisture Density Curve.....	46
Figure B.1 Topeka 100% Cement Freeze-Thaw Trend .....	47
Figure B.2 KC 100% Cement Freeze-Thaw Trend .....	47
Figure B.3 Topeka 50% Cement 50% Fly Ash Freeze-Thaw Trend.....	48
Figure B.4 KC 50% Cement 50% Fly Ash Freeze-Thaw Trend .....	48
Figure B.5 Topeka 35% Cement 65% Fly Ash Freeze-Thaw Trend.....	49
Figure B.6 KC 35% Cement 65% Fly Ash Freeze-Thaw Trend .....	49
Figure B.7 Topeka RCA and Control Comparison.....	50
Figure C.1 Topeka Control 100% Cement Moisture Density Curve.....	51
Figure C.2 KC Control 100% Moisture Density Curve.....	51
Figure C.3 Topeka Control 50-50 Moisture Density Curve .....	52
Figure C.4 KC Control 50-50 Moisture Density Curve.....	52
Figure D.1 Topeka Control 100% Cement Freeze-Thaw Trend.....	53
Figure D.2 KC Control 100% Cement Freeze-Thaw Trend.....	53
Figure D.3 Topeka Control 50-50 Freeze-Thaw Trend .....	54
Figure D.4 KC Control 50-50 Freeze-Thaw Trend .....	54
Figure E.1 Topeka 100% Cement Comparison .....	55
Figure E.2 KC 100% Cement Comparison.....	55

Figure E.3 Topeka 50-50 Comparison.....	56
Figure E.4 KC 50-50 Comparison .....	56
Figure E.5 Topeka & KC 35-65 Comparison .....	57

## **List of Tables**

Table 3-1: Sieve Analysis of All Aggregates .....	17
Table 3-2: Coarse Aggregate Properties .....	18
Table 3-3: Fine Aggregate Properties .....	18
Table 3-4: Mill Test Results for Cement used in Cement Treated Base .....	19
Table 3-5: Mill Results for Fly Ash used in Cement Treated Base .....	20
Table 4-1: Blend Proportions for Cement Treated Base Mixtures .....	21
Table 4-2: PCTB Blend Design % Binder and Compressive Strength.....	24
Table 5-1: Summary of D-Cracked RCA Mass Change Results .....	30
Table 5-2: Summary of D-Cracked RCA RDME Results .....	31
Table 5-3: Summary of D-Cracked RCA Length Change Results .....	32
Table 6-1: Average UCS of Control Samples.....	35
Table 6-2: Summary of Control Mass Change Results .....	36
Table 6-3: Summary of Control RDME Results.....	36
Table 6-4: Summary of Control Length Change Results.....	37

## **Acknowledgements**

I would like to thank my advisor, Dr. Christopher Jones, for providing guidance and support through this project. Thank you to Dr. Mustaque Hossain and Dr. Stacey Kulesza for serving on my advisory committee.

I would also like to thank Cody Delaney and Ben Thurlow in the civil engineering department research technologists, for assisting with any and all equipment maintenance.

Also, thanks to Bayer Construction, Central Plains Cement, Midwest Concrete Materials for donating the materials for the project.

Finally I would like to thank Masoumeh Tavakol and Yadira Porras for assisting with experimental portions of this project as well as any fellow students who assisted when called upon.

# **Chapter 1 - Introduction**

## **1.1 Background**

D-cracking, or durability cracking, is a progressive structural deterioration of the concrete. It is caused by freezing and thawing, beginning in coarse aggregate. It starts below the surface of pavement at joints that permit moisture intrusion and progresses inward and upward. D-cracking has caused damage worth millions of dollars to Kansas concrete pavements over the last century. Kansas concrete pavements, which commonly consist of limestone, are highly susceptible to D-cracking when subjected to freeze-thaw conditions. To test the durability of mixtures for aggregate in concrete pavements, the Kansas Department of Transportation (KDOT) follows two procedures to predict freeze-thaw performance in the field. The first method, KTMR-21 (KDOT, 1999), determines aggregate resistance to disintegration by freezing and thawing. The second method known as KTMR-22 (KDOT, 2015b), is a modified version of ASTM C666 (ASTM, 2015c). It consists of a 90-day concrete curing period, with a 21-day drying period after an initial 67 days curing in 100% humidity. Dry curing removes additional moisture that would cause damage during freezing. The lower degree of saturation causes less deterioration during the three months of freeze-thaw cycling required by KTMR-22 than that would be experienced at a higher degree of saturation. The combined durations of KTMR-22 curing and freeze-thaw testing yield a six-month aggregate qualification procedure.

## **1.2 Problem Statement**

Recycled concrete aggregate (RCA) obtained from recycling Portland cement concrete Pavements (PCCP) can be used as coarse or fine aggregates in concrete pavements. However, concrete incorporating more than about 10 to 20 percent fine aggregates from RCA will have higher water demand for a given slump resulting in lower quality. On large projects or projects where suitable quality aggregate is not readily available, on-site processed RCA can result in economy. However, not much information is available about the suitability of lower quality recycled PCCP aggregates such as those from the pavements with “D” cracking.

### **1.3 Objectives**

The primary objectives of this study were as follows:

1. Determine freeze thaw durability of RCA aggregates using KTMR-21
2. Determine strength of portland cement treated base (PCTB) incorporating RCA
3. Determine the freeze thaw durability of PCTB incorporating RCA
4. Compare durability of PCTB incorporating RCA to that of control samples using virgin aggregate

### **1.4 Study Method**

This study was divided into two separate parts. The first part, denoted as “D-cracked RCA cement treated base study,” consists of tasks developed to meet objectives 1 and 2. For the study, RCA from D-cracked pavements was obtained from sources in Topeka and Kansas City. These aggregates were used to batch 3 different base mixes per aggregate source. All mixes followed KDOT’s 90-day curing outlined in KTMR-22. This entailed 67 days in a 100% moisture room, followed by drying in a 73°F room at 50% relative humidity for 21 days. After 88 total days of curing, the samples were immersed in 70°F water for 24 hours followed by immersion in 40°F water. Upon completion of curing, all samples were subjected to cycles of freezing in air and thawing in water in accordance with ASTM C666 Procedure B (ASTM, 2015c). Multiple measurements of each sample’s mass, relative dynamic modulus of elasticity (RDME), and length change were recorded.

The second part of the study was to compare the RCA samples to control samples. The control samples consisted of virgin aggregate that had not been previously used in any concrete mixing. The control aggregate and mixtures were placed under the exact same conditions of the RCA as to limit any variability.

### **1.5 Thesis Outline**

Chapter 2 consists of a literature review with information regarding freeze-thaw damage in aggregates in concrete, procedures for identifying durable aggregates, effects of drying methods, and modified versions of standard curing and freeze-thaw testing methods used by different departments of transportation around the United States of America. In Chapter 3, the

materials used for the batching of the treated base are discussed. Chapter 4 provides explanations of the methods that were followed in the study. Chapters 5 and 6 provide the results of the RCA and control studies. A discussion of all results is provided in Chapter 7, followed by conclusions and recommendations in Chapter 8.

## **Chapter 2 - Literature Review**

### **2.1 Recycled Concrete Aggregates (RCA)**

Recycled Concrete Aggregates (RCA) are the product of the demolition of concrete pavements or structures. Portland cement concrete pavements (PCCP) a 100 percent recyclable material (Verian et al. 2013). RCA is categorized by a minimum of 90%, by mass, from Portland cement-based wastes and natural aggregates (Silva et al. 2016). The use of RCA in construction is considerable in the building industry around the world. In Great Britain, 10% of used aggregates are RCA; in Holland, 78,000 tons of RCA were used in 1994 (Oikonomou, 2005). The properties of fresh or hardened concrete consisted of 20% of coarse RCA has shown no difference as compared to conventional concrete. In addition, Germany has been aiming for 40% recycling of building waste since 1991 (Oikonomou, 2005).

#### ***2.1.1 Physical Properties of RCA***

There has been an abundance of research on evaluating physical properties of RCA. RCA particles are formed often from pavement, removing any reinforcement and crushing to a specific size and gradation (E701, 2016). While up to 100 percent of the coarse aggregate can be recycled material, the percentage of fine aggregate is usually limited to 10 to 20 percent (E701, 2016). It is possible to achieve almost any gradation with recycled materials. While the crushing operation may leave some residual dust on the aggregate surfaces, this does not pose a problem in most cases. The crushed material has a lower relative density than virgin material. Usually, recycled coarse aggregate has a specific gravity of 2.2 to 2.5 in the saturated surface-dry (SSD) condition. As the size decreases, so does the relative density. Recycled sand has a relative density of approximately 2.0 to 2.3 SSD (E701, 2016). This is due to absorption is much higher due to the cement mortar attached to particles. It is typically 2 to 6 percent for coarse aggregate and higher for sands. This can affect the workability of the concrete mixture. Abrasion loss is not a concern for recycled aggregate; nor is sulfate soundness. Residual chlorides in a mixture, as from application of deicing salts to a pavement, are usually below threshold values for both fine and coarse aggregates and are not a concern (E701, 2016).

### ***2.1.2 RCA Production***

RCA is produced by crushing and sorting existing concrete and producing desired aggregate sizes. The recycling process normally uses primary and secondary crushing stages. In the primary crushing stage, Jawcrushers are typically used to provide the best size distribution and reducing the material size down to about 3 to 4 in. A secondary crushing is done to achieve desired maximum coarse aggregate size, as well as more round and less angular particles (Silva et al. 2016) Three main types of crushers used in concrete recycling are jaw, cone, and impact designs, which differ in how they crush the concrete. Different crushing processes remove different amounts of mortar from the original aggregate particles. The type of crushing devices used to break down larger pieces and the number of processing stages influences the size and shape of the resulting aggregates (Verian et al. 2013).

## **2.2 D-Cracking of Coarse Aggregate**

D-cracking occurs in coarse aggregate that has been subjected to cycles of freezing and thawing. Although it has been experienced since the 1930s when concrete pavements first came into general use, there is little agreement on the term's origin or the meaning of the 'D' which variously denotes 'distress, discoloration, or deterioration,' or the shape of the pieces that break off from the pavement (O'Doherty, 1987). D-cracking starts out of sight at the base of the slab near the joints. It can take several years to progress up to the top of the slab where it first becomes visible (O'Doherty, 1987).

### ***2.2.1 Mechanism of D-Cracking***

D-cracking is related to moisture with the presence of freezing conditions. Aggregates that cause D-cracking absorb moisture from the pavement base and from surface water entering through cracks and joints. If aggregate pores are full when freezing occurs, internal pore pressure cracks the particles causing the mortar to crack as well. More cracks develop with repeated freezing and thawing cycles (Whitehurst, 1980). Water expands approximately 9% upon freezing. If any given capillary space is greater than 91.7% filled, the volume of ice will be greater than the volume of pore space and pressure will develop as the ice crystal outgrows the cavity (Thompson, Olsen, & Dempsey, 1980). Powers and Helmuth (1953) proposed the ice

accretion/osmotic pressure theory to explain experimental results that were inconsistent with the hydraulic pressure theory. The osmotic pressure theory states that, during freezing, water moves from the gel pores to the capillary pores according to laws of thermodynamics and the theory of osmosis (Powers & Helmuth, 1953). During this process, a concentrated alkali solution develops as ice is produced. Unfrozen water travels toward the freezing site due to differences in solute concentrations.

### ***2.2.2 Appearance and Progression of D-Cracking***

D-cracking is initiated by moisture, usually at the bottom of a slab, where contact with the base inhibits drying. It is accentuated by cracks and joints providing paths for water to the base and by the presence of poor drainage. The moisture penetrates the tiny pores in the particles of certain types of coarse aggregates (O'Doherty, 1987). D-cracking normally appears at transverse-longitudinal joint intersections, and occasionally at the intersection of longitudinal joints and transverse cracks and at the outside corners of a pavement slab (Whitehurst, 1980). As cracking progresses along the joints, the resulting crack pattern forms a nearly continuous network that is confined to the peripheral areas of the slab. With continued deterioration, the pattern encroaches rapidly on the remaining portion of the slab (Whitehurst, 1980). Generally, it takes several years to progress upward to the top of the slab where it first becomes visible as a series of small cracks, often preceded and accompanied by dark discoloration of the concrete surface. It is usually not detected in the early stages except by core drilling (O'Doherty, 1987).

### ***2.2.3 Conditions for D-Cracking***

Three basic conditions are needed to produce D-cracking. First, as stated in Section 2.1.1, moisture must be present and available so that the particles are more than 91.7% saturated. Second, the particles of coarse aggregate must be susceptible to cracking. Limestones and fine-grained sedimentary rocks are notorious for having planes-of-weakness and deleterious pore sizes (0.4 to 2.0 microns). The larger the particle, the longer the water path, and the more cracks will form. Third, there must be freezing and thawing—the problem is less prevalent in very cold regions where fewer cycles of freezing occur (O'Doherty, 1987). Not all sedimentary aggregates cause the problem. Aggregates with low permeability, high porosity, and small pore size are most likely to cause D-cracking (Schwartz, 1987).

### ***2.2.4 Non-influential Factors***

A study conducted at the University of Illinois determined that the use of entrained air all but eliminated problems of freeze-thaw deterioration of cement paste (Thompson, Olsen, & Dempsey, 1980). In addition, fine aggregate properties, type and amount of cement, pavement design, and traffic have little influence on D-cracking (Schwartz, 1987). A positive underdrain system isn't sufficient to prevent D-cracking from developing. It can only postpone it (Schwartz, 1987).

### ***2.2.5 Prevention***

To avoid using D-cracking-susceptible aggregates, some states take a source acceptance approach. Acceptance criteria include performance histories and results of extensive testing. Besides approving general source locations, highway agencies may even identify specific acceptable ledges within a source for crushed stone (Schwartz, 1987). Aggregates, such as high quality dolomite and rocks of igneous origin are not as prone to cracking, while aggregates with high proportions of chert and limestone are at a greater risk. Improvement in drainage of the base and sealing of joints pay significant dividends in performance but cannot prevent deterioration (O'Doherty, 1987). Mechanical separation can be utilized to separate aggregates on the basis of their mechanical properties or by specific gravity. Separation by specific gravity is the most common method. Heavy fluids are used to float off materials with specific gravities lower than the specified amount, typically 2.5. The assumption behind using heavy media separation to improve aggregate quality is that particles with low specific gravities are less durable than particles with high specific gravities (Thompson, Olsen, & Dempsey, 1980).

## **2.3 Freeze-Thaw Resistance of Concrete**

In addition to durable aggregate for adequate freeze-thaw performance, a durable cement paste matrix is needed as well. The mechanisms of internal damage, surface scaling to hardened cement paste, and drying are discussed in this section.

### ***2.3.1: Mechanisms of Internal Damage***

If the aggregates used in concrete are frost-resistant, the freeze-thaw resistance of the cement paste determines the overall resistance of the concrete to freezing and thawing. If the aggregate is susceptible to freeze-thaw damage, it can contribute to concrete deterioration. Several theories have been proposed to explain concrete damage due to freezing and thawing (FHWA, 2006).

Similarly as in *2.2.1 Mechanism of D-Cracking*, the critical saturation theory, proposed by Powers, states that concrete will only suffer damage from freezing when the capillaries in the cement paste are more than 91.7 percent full of water (Powers, 1945). This theory is based on the fact that water expands in volume by approximately 9 percent when it freezes. If the capillary pores are saturated with water and the water freezes, stresses will be generated. If the pores are only partially filled, the expansion resulting from ice formation may be accommodated (FHWA, 2006).

The hydraulic pressure theory, also put forth by Powers, states that damage from freezing is caused by a buildup of hydraulic pressure from the resistance to flow of unfrozen water in cement paste capillaries. As water freezes, if the cement paste does not expand to accommodate it, unfrozen water will be pushed through the capillary pores, away from the sites of freezing. It is like that of water flowing through a pipe (Powers, 1949). The theoretical concept of soil suction was developed in soil physics in the early 1900s. The soil suction theory mainly developed in relation to the soil-water-plant system. The importance of soil suction in explaining the mechanical behavior of unsaturated soils relative to engineering problems was introduced at the Road Research Laboratory in England (Fredlund & Rahardjo, 1993). The soil suction as quantified in terms of relative humidity is commonly called “total suction.” It has two components, namely, matric and osmotic suction. In soils, the pores with small radii act as capillary tubes that cause the soil water to rise above the water table. The capillary water has a negative pressure with respect to the air pressure, which is generally atmospheric pressure (Fredlund & Rahardjo, 1993). At low degrees of saturation, the pore-water pressures can be highly negative with values as low as minus 7,000 kPa.

### ***2.3.2: Effects of Surface Scaling***

Compared to internal cracking, scaling is only a surface effect, however it is the most apparent form of deterioration. It usually only occurs when the concrete freezes in water and is amplified by the use of deicer salts (Pigeon, Pleau, & Aitcin, 1986). When deicer salt particles come into contact with water, the freezing point is lowered. As a result, an increase in deicing chemicals corresponds to a reduction in pressure due to the formation of ice. However, chloride ions in deicing salts can become physically or chemically bound by cement hydration products and can cause concrete expansion (Wu, Shi, Gao, Wang, & Cao, 2015). Other factors can cause scaling to take place. Excessive bleeding, bad finishing procedures, plastic shrinkage cracking, overworking of the surface during the finishing operations, lack of curing, and early exposure to relatively high temperature can all weaken the concrete surface and be an indirect cause of rapid scaling when concrete is exposed to freezing in water (Pigeon & Pleau, 1995). Loss of mass during freeze-thaw is mostly caused by surface scaling, but it can increase significantly when severe internal cracking begins to disintegrate the test specimens. Proper air entrainment will improve the concrete performance in deicer salt scaling, but will not prevent scaling in concrete with a high water-to-cement ratio (Pigeon, Pleau, & Aitcin, 1986). High water-to-cement ratio causes a high paste permeability and low strength. As a result, air entraining is not effective in reducing surface scaling.

### ***2.3.4: Effect of Drying***

Periods of drying concrete can be very beneficial for freeze-thaw durability. Drying causes the pores in the concrete to become enlarged and to become more interconnected which increases permeability. This increased water permeability will allow water to reenter the concrete faster than before the drying period (Pigeon & Pleau, 1995). As a result, drying eliminates the threat of internal damage caused by the expansive pressures of freezing water. However, if the concrete is once again exposed to water for an extended period of time, the benefits of the drying will no longer be available. The re-saturation of the pore network has been shown to be a more energy intensive and slower process due to the different flow characteristics of the partially dried concrete (Sellier et al. 2011). For intermediate re-saturation times, the implication of the slower re-saturation is a net increase in freeze thaw resistance due to partial saturation of the pore network.

## **2.4 Durable Aggregate and Concrete Identification Procedures**

Many standard test methods have been developed by American Society for Testing and Materials (ASTM) and other organizations to measure and predict freeze-thaw behavior of aggregate and concrete. Two concrete mixture test methods and three aggregate test methods are discussed in this chapter. As D-cracking is more critical in aggregate, it is of most importance to identify aggregates suitable for freeze-thaw.

### ***2.4.1 KTMR-21: Soundness & Modified Soundness of Aggregates by Freezing and Thawing***

KTMR-21 is a standard used by KDOT to determine aggregate resistance to disintegration by freezing and thawing (KDOT, 1999). The procedure is for Class 1 Aggregates or Official Quality Aggregates, including Official Quality Sand-Gravel. The procedure is for coarse aggregates and requires a design gradation for the testing. The design gradation is determined by the gradation of the coarse aggregate. The procedure for testing begins with a soaking period. After soaking, the material, while in a saturated and drained condition, is placed in freezing equipment that maintains a temperature between -20 and 0°F (KDOT, 1999). The sample remains in the freezing equipment until frozen, but in no case shall the period of time be less than two hours. The aggregate is then placed in a tap water bath maintained at 70-80°F for a period of 40 minutes. One freezing period and one thawing period is considered one cycle. The test concludes after 25 cycles. The aggregate is washed over a #12 sieve and the freeze-thaw loss ratio is calculated by dividing the cumulative mass of the sample at the end of the test by the cumulative mass of the sample at the beginning of the test. The aggregates must have a loss ratio of 85 or better to be tested under KTMR-22

### ***2.4.2 ASTM C666: Rapid Freezing and Thawing of Concrete***

*ASTM C666: Standard Test Method for Resistance of Concrete to Rapid Freezing and Thawing*, is the standard method used by the majority of transportation organizations to test freeze-thaw resistance of concrete. It provides the procedure for freeze-thaw testing of concrete specimens as well as the procedure for determining the specimen's durability. There are two procedures within ASTM C666. Procedure A requires the samples to be immersed in water

during the freeze thaw process while Procedure B uses air to freeze the samples followed by thawing in water. Each cycle of freeze-thaw must last between two and five hours. The temperature at the center of the concrete specimens must be  $40\pm 3^{\circ}\text{F}$  at the beginning of each cycle. The temperature is then lowered to  $0\pm 3^{\circ}\text{F}$  and then raised back to  $40\pm 3^{\circ}\text{F}$  at the end of the cycle (ASTM, 2015c).

Durability readings must be recorded for concrete specimens once every 36 cycles or less. If a sample is suspected of degrading quickly, readings may be taken at shorter intervals. ASTM C666 requires mass and resonant frequency be measure at every interval. Mass loss is typically attributed to surface scaling or internal cracks forming within the samples. Mass gain can be observed and is attributed to a sample absorbing water into its pores. Another factor to mass gain may be the cement is still hydrating. However, the stiffness of the samples is affected more so. The resonant frequency of a concrete specimen is the natural frequency at which the maximum amplitude of an induced mechanical wave occurs. The initial frequency is measured before the samples have been subjected to freeze-thaw and then is monitored at each interval. The specimen's relative dynamic modulus of elasticity (RDME) is a calculation based on the resonant frequency and as a result, is proportionally related to the resonant frequency. When the RDME reaches 60%, mass and frequency readings will cease and the final number of freeze-thaw cycles will be documented. However, ASTM C666 allows other failure limits to be specified. Explanation of obtaining a specimen's resonant frequency and how to calculate will be discussed in Chapter 4.

ASTM C666 also provides and optional length change procedure which may be conducted every interval of testing to determine the durability of the specimens. When internal cracks form in aggregate or in paste, the volume increases and the volume expands. This coupled with the cycling of freezing and thawing will eventually cause failure of the sample. ASTM C666 suggests using an expansion of 0.10% of a specimen's original length as a failure limit. The procedure for determining the expansion will be discussed in Chapter 4.

### ***2.4.3 ASTM C88: Aggregate Sulfate Soundness***

The aggregate sulfate soundness test method covers the testing of aggregates to estimate their soundness when subjected to weathering action in concrete or other applications. This is accomplished by repeated immersion in saturated solutions of sodium or magnesium sulfate

followed by oven drying to partially or completely dehydrate the salt precipitated in the permeable pore spaces. The internal expansive force, derived from rehydration of the salt upon re-immersion, simulates the expansion of water upon freezing (ASTM, 2013). This test is useful when aggregate has no known performance records or when little to no information is available.

#### ***2.4.4 ASTM C295 Petrographic Examination of Aggregates for Concrete***

ASTM C295 details procedures for petrographic examination of materials proposed for aggregates. The procedures may involve microscopy, x-ray diffraction analysis, infrared spectroscopy, and differential thermal analysis. The test must be conducted by an experienced petrographer. The purpose of the examination is to determine the physical and chemical characteristics of the material intended to be used. The examination can identify the portion of each coarse aggregate that is composed of weathered particles and the extent of the weathering. This is especially important for aggregates that will be exposed to freezing and thawing as finely porous and highly weathered or otherwise altered rocks are susceptible to damage by freezing and thawing.

#### ***2.4.5 Washington Hydraulic Fracture Test***

The Washington Hydraulic Fracture Test (WHFT) is used to predict aggregate freeze-thaw performance by inducing pressure in aggregate pore walls to simulate the expansion of water due to freezing and thawing. The procedure is to use compressed nitrogen to force water into the pores of the aggregate. Then the pressure is released to allow for expansion of the air within the pores. Water is expelled as a result and induces an internal stress on the pore walls similar to that of freezing and thawing. The pore walls will fracture when the structure of the wall cannot dissipate the pressure fast enough. The severity can be used to predict the freeze-thaw resistance of the aggregate (Embacher & Snyder, 2003).

### **2.5 Curing Methods for Freeze-Thaw Testing**

Higher resistance to physical and chemical deterioration is the primary goal of an effective concrete curing process. Specimen curing typically involves a lime-water bath or a moisture room for a specified time. Two unconventional curing methods such as microwave and steam curing as well as temperature-match-curing are discussed in the sections below.

### ***2.5.1 Microwave and Steam Curing***

A study conducted at the Chaoyang University of Technology in Taichung County, Taiwan, used microwave and steam curing of specimens to test the freeze-thaw resistance. The concrete specimens were made with Type I Portland cement, Class F fly ash, a ground blast-furnace, and a silica fume. Two steam-curing temperatures (65 and 75° C) and one curing time (7h) were used in the investigation. The samples were submerged in water for 17 hours after demolding (Lee, 2007). A microwave oven with 700 W power was used to microwave cure the other concrete specimens. The specimens were placed in a glass container with 1,000 mL of water in it, and the container was placed in the microwave for four separate treatments (0, 20, 40, and 60 mins) (Lee, 2007).

The freeze-thaw cycles were applied at a rate of one cycle per 185 min with 1.5 h of freezing in air at -18°C followed by 1.5 hr. of thawing in wet air at +4.4°C. The procedure follows very closely to ASTM C666 Procedure B.

The freeze-thaw test results show that both steam-cured and steam–microwave cured samples had slightly lower initial relative dynamic modulus values as compared with the concrete that was water cured for 28 days. Therefore, for the conditions used in this study, the steam– microwave curing of the concrete had little effect on the concrete freeze-thaw durability. The microwave-cured concrete did not show an increase in deterioration relative to the concrete that was steam cured but showed an increase in strength development (Lee, 2007).

### ***2.5.2 Temperature-Match-Curing***

High-strength concrete (HSC) in large structures typically has high cement content and may develop high internal temperatures due to cement hydration. An experiment in which concrete freeze-thaw specimens were cured under temperature conditions that matched those of in situ concrete was created by Jonsson and Olek in 2004. This technique, called temperature-match-curing (TMC), ensures that concrete test samples experience the same temperature history as the concrete member they represent (Jonsson & Olek, 2004).

Four different mix designs were utilized in this study. Each mixture contained Type I cement, a 0.33 water-cement-ratio, and no Air Entraining Admixture (AEA). The procedure was to use 5.5 liters of the mix and place them in separate polystyrene blocks which were meant to simulate actual temperature profiles induced in HSC members. The concrete temperature inside

the block was continuously monitored with thermocouples, and collected temperature information was used to simultaneously temperature-match-cure (TMC) a series of freeze-thaw specimens (Jonsson & Olek, 2004). For each mixture, four freeze-thaw prisms were prepared. Half of the specimens were temperature-match-cured for 2 days, and the other half of the specimens were cured at room temperature. At the end of the initial 2-day curing period, the specimens were demolded and moved to a fog room (Jonsson & Olek, 2004).

Freeze-thaw conditions were conducted in accordance with ASTM C 666 Procedure A. The TMC specimens outperformed the control specimens for all four mixtures. When the control specimens started to deteriorate, complete deterioration usually occurred within a relatively few freeze-thaw cycles. The RDME usually dropped from 90% to below 60% in a single set of 30 cycles. The rate of deterioration was considerably more gradual for the TMC specimens than that of the control specimens. The relative performance of the TMC specimens ranged from 3 to 217% over the control specimens (Jonsson & Olek, 2004).

## **2.6 Modified Versions of ASTM C666**

Several state Departments of Transportation (DOT) use ASTM C666 to find aggregate and concrete suitable for freeze-thaw. However, since the regions of these DOTs happen to differ, some of the organizations have modified the tests to obtain results that correlate well with field records.

### ***2.6.1 Kansas Department of Transportation***

The standard test that KDOT utilizes to determine aggregate is KTMR-22. It outlines the curing and testing procedures for concrete specimens subjected to ASTM C666 Procedure B. Procedure B utilizes air freezing and immersion in water to thaw. The specimens undergo a 90-day curing method, which entails 67 days curing in a 100% moisture room. The specimens are then transferred to a curing room at 50% humidity for 21 days followed by full immersion in water for 2 days. The two months in the moisture room allows extensive cement hydration. This leads to a more durable past matrix. The extensive moist curing period is used so that the damage from the freeze-thaw primarily occurs in the coarse aggregate. The 21 day period of dry curing removes excess moisture from the aggregate pores which will reduce the expansive pressures caused by freezing water.

KDOT has also modified the maximum number of cycles from ASTM C666 from 300 to 660. When tests were only conducted through 300 cycles, the results were not accurately predicting the performance in the field. KDOT selected 660 cycles based on weather data and pavement service life. Weather data shows that Kansas experiences 33 freeze-thaw cycles per year and the expected service life of a pavement is 20 years. Multiplying 33 by 20 gives 660, the number of cycles specified in KTMR-22. Aggregate is deemed durable if the samples maintain an expansion  $\leq 0.025\%$  and a RDME  $\geq 95\%$  after the completion of 660 cycles (KDOT, 2015b).

### ***2.6.2 Other Organization's Methods***

The Michigan Department of Transportation (MDOT), uses ASTM C666 Procedure B similarly to KDOT. However, MDOT specifies a 14-day curing period. The samples are covered with a wet burlap for the first 24 hours after casting. The samples are then demolded and immersed in saturated lime water for 12 days before being placed in 40°F water for 16 hours. Differently from KDOT, MDOT uses only 300 cycles or until expansion reaches 0.10%. MDOT does not require measurement of mass or RDME (MDOT, 2015).

The Ohio Department of Transportation (ODOT) uses ASTM C 666 Procedure B. The difference with the ODOT procedure is the samples are cured by being placed in a moisture room for 24 hours while still within the molds. The samples are then demolded and immersed in water for 14 days (Woodhouse, 2005). ASTM C 666 must be performed on all  $\frac{3}{4}$ " and 1" nominal aggregate. Aggregate durability is determined through calculation of the area under the curve obtained by plotting expansion versus the number of freeze-thaw cycles for a given test specimen. For aggregate sources that are approved by ODOT within a year of testing, this area may not exceed 2.05 after a maximum of 350 cycles. Between one and two years after approval, this area may not exceed 1.00 after 350 cycles (ODOT, 2013).

## **2.7 Summary**

Internal damage to concrete from freeze-thaw occurs due to the development of hydraulic pressures in the pores of the cement. If the surface of the concrete is exposed to water and deicing chemicals, it is likely it will be susceptible to surface scaling. Many standard test procedures have been developed to predict and measure the durability of aggregate and concrete exposed to freeze-thaw conditions. KDOT's method uses an extended curing period, more than double the cycles specified by ASTM C 666 Procedure B, and a more stringent RDME

acceptance criteria. Due to the longer curing, higher number of cycles, and higher RDME acceptance criteria, KDOT's standards are more stringent than those of other DOT's. Other states such as Michigan and Ohio have adopted modified curing methods, freeze-thaw test durations, and performance criteria based on ASTM C 666. Curing studies have shown that elevation of the temperature during curing can accelerate deterioration of concrete. However, even though the studies are to simulate field conditions, they show that exposing concrete to drying periods during curing yield higher durability after several freeze-thaw cycles.

## Chapter 3 - Materials

For this study, two different sources of D-cracked recycled concrete aggregate (RCA) from D-cracked pavements were used to test the freeze-thaw durability. The first source of RCA was taken from a piece of a roadway named Topeka Boulevard in Topeka, KS. The second source was taken from the runway reconstruction at the Kansas City International Airport. The information on the Topeka aggregate is not known, however the KC aggregates, quarried from the Martin-Marietta Sunflower Quarry, consist of limestone (calcium carbonate) with minor clay minerals (aluminum silicates). There is a possibility of also minor dolomite (magnesium carbonate) within the aggregate as well. The two RCA sources were split into coarse and fine aggregates based on the washed sieve analysis following Kansas Test Method KT-2 (KDOT, 2016a). In addition to the RCA, a source of virgin coarse aggregate and fine aggregate were obtained to create control samples to compare the performance of the specimens. The virgin coarse aggregate was provided by a local supplier, Midwest Concrete Materials (MCM). All sources of aggregate were first subjected to the Los Angeles abrasion test (ASTM, 2014), to ensure the aggregate was suitable for pavement applications. The next step was to determine the freeze-thaw durability of base aggregates, KTMR-21 (KDOT, 1999), was the test method to determine the durability of these aggregates. Table 3-1 shows the sieve analysis for the RCA as well as the virgin aggregates used in the control PCTB.

**Table 3-1: Sieve Analysis of All Aggregates**

Aggregate Source	1.0in	3/4in	1/2in	3/8in	#4	#8	#40	#100	#200
KC	0	6.2	27.4	40.9	62.2	72.7	94.4	94.5	100
Topeka	0	6.2	21.6	35.1	56.8	68.3	92.4	97.2	100
CS-2	0	0	0	0.2	0.5	32.9	65.3	90.8	100
CA-5	0	4.9	42.7	67.4	95.6	98.8	98.8	98.8	100

### 3.1 Coarse Aggregate

Aggregate properties such as saturated surfaced dry (SSD) bulk specific gravity and absorption were needed for preliminary analysis of the types of aggregate within the RCA. These

values were obtained in accordance with ASTM C127: Standard Test Method for Density, Relative Density (Specific Gravity), and Absorption of Coarse Aggregate (ASTM, 2015d). Aggregate was immersed in water for 24 hours in order to saturate the pores. The coarse aggregates were then towel-dried and weighed in SSD condition. The SSD aggregate's apparent mass in water was then obtained before recording its mass after oven-drying for 24 hours. The SSD bulk specific gravity was determined through comparison of the SSD and apparent masses. Absorption was found by comparing the SSD and oven-dry masses (ASTM, 2015d). Aggregate properties for the coarse aggregate portion of the RCA are displayed in Table 3-2.

**Table 3-2: Coarse Aggregate Properties**

Aggregate Source	SSD Bulk Specific Gravity	Absorption (%)	La Abrasion (%)	KTMR-21
Topeka RCA	2.39	5.71	32.0	0.96
Kansas City RCA	2.52	2.89	52.0	0.94
Midwest Concrete Materials-Coarse Aggregate (CA-5)	2.61	2.86	33.7	0.97

### 3.2 Fine Aggregate

Using the gravimetric procedure outlined in ASTM C128: Standard Test Method for Density, Relative Density (Specific Gravity), and Absorption of Fine Aggregate (ASTM, 2015a), the properties of the fine aggregate portion of the RCA were determined. The fine aggregate was tested by immersing it in water for 24 hours then dried to SSD condition. The surface moisture was tested by placing in a cone-shaped mold with two open ends. A tamper was used to consolidate the aggregate and was considered SSD when it deformed slightly upon removal of the mold. Table 3-3 provides the properties of the fine aggregates.

**Table 3-3: Fine Aggregate Properties**

Aggregate Source	SSD Bulk Specific Gravity	Absorption (%)
Topeka RCA	2.02	5.71
Kansas City RCA	2.45	2.89
KDOT Fine Aggregate (CS-2)	2.51	3.69

### 3.3 Cement

Type I/II cement from Central Plain Cement Company was used in all PCTB mixes in accordance with KTMR-22 specifications (KDOT, KTMR-22: Resistance of Concrete to Rapid Freezing and Thawing, 2015b). The average chemical and physical compositions of the cement are shown in Table 3-4.

**Table 3-4: Mill Test Results for Cement used in Cement Treated Base**

Property	Spec Limit	Reported Value	
SiO <sub>2</sub> (%)	None	20.2	
Al <sub>2</sub> O <sub>3</sub> (%)	6.0 max	4.7	
Fe <sub>2</sub> O <sub>3</sub> (%)	6.0 max	3.1	
CaO (%)	None	64.0	
MgO (%)	6.0 max	1.2	
SO <sub>3</sub> (%)	3.0 max	3.0	
Loss on ignition (%)	3.5 max	2.6	
Insoluble residue (%)	1.5 max	0.27	
CO <sub>2</sub> (%)	None	1.8	
Limestone (%)	5.0 max	4.5	
CaCO <sub>3</sub> in Limestone (%)	70 min	93	
Adjusted Potential Phase Compositions (C150)	C3S (%)	None	55
	C2S (%)	None	17
	C3A (%)	8 max	7
	C4AF (%)	None	9
	C3S+4.75C3A (%)	100 max	90
Air content of mortar (%)	12 max	8	
Blaine Fineness (m <sup>2</sup> /kg)	260 – 430	361	
-325 (%)	None	95.8	
Autoclave expansion (%)	0.80 max	-.01	
Compressive Strength	1 day	None	2140
	3 days	1740 min	3800
	7 days	2760 min	5060
	28 days	None	7050
Time of setting (minutes)	45 – 375	97	
Mortar Bar Expansion (%)	0.020 max	0.005	
Specific Gravity	None	3.15	

### 3.4 Fly Ash

Class C fly ash from Kansas City FlyAsh, LLC was used as a pozzolan for PCTB mixtures that were designed for fly ash and cement. Class C was chosen as it has some cementitious properties and added to the 7-day compressive strength of the specimens. The average chemical and physical compositions of the fly ash used for the study are shown in Table 3-5

**Table 3-5: Mill Results for Fly Ash used in Cement Treated Base**

Property	Value	ASTM C 618 Class C	AASHTO M295 Class C
SiO <sub>2</sub> (%)	35.70	None	None
Al <sub>2</sub> O <sub>3</sub> (%)	18.90	None	None
Fe <sub>2</sub> O <sub>3</sub> (%)	6.12	None	None
SiO <sub>2</sub> +Al <sub>2</sub> O <sub>3</sub> +Fe <sub>2</sub> O <sub>3</sub> (%)	60.72	50 min	50 min
CaO (%)	26.24	None	None
MgO (%)	5.14	None	None
SO <sub>3</sub> (%)	1.93	5.0 max	5.0 max
Moisture content (%)	0.06	3.0 max	3.0 max
Loss on ignition (%)	0.43	6.0 max	5.0 max
Na <sub>2</sub> O (%)	1.47	None	None
K <sub>2</sub> O (%)	0.47	None	None
325 Sieve, % Passing	8.2	34 max	34 max
Density	2.61	None	None
Strength Activity Index with Portland Cement at 7 days (%)	103	None	None
Water Requirement (%)	94	105 max	105 max
Autoclave expansion (%)	0.07	0.8 max	0.8 max

## Chapter 4 - Methods

### 4.1 PCTB Mix Design

All PCTB mixes were based on the optimum moisture content and density curve requirements outlined in KT-37. A minimum of four points were needed to determine the optimum moisture for each different blend of PCTB. The 7-day unconfined compressive strength (UCS) of the PCTB specimens was to be in the range of 650 psi-1600 psi (KDOT, 2015a). Mixture proportions for each mixture are summarized in Table 4-1. Addition of a pozzolan in the form of Class C fly ash was utilized to increase the paste content of the samples without greatly increasing the compressive strength. It is shown that binder content has the greatest sensitivity to the performance of specimens in freeze-thaw (Ashraf et al. 2018).

**Table 4-1: Blend Proportions for Cement Treated Base Mixtures**

PCTB Blend	RCA (%)	Cement (%)	Class C Fly Ash (%)
Topeka 100%-Cement	93	7	*
Topeka 50%-Cement 50%-Fly Ash	91	9	*
Topeka 35%-Cement 65% Fly Ash	90	5	5
Kansas City 100%-Cement	88	6	6
Kansas City 50%-Cement 50%-Fly Ash	86	4.9	9.1
Kansas City 35%-Cement 65%-Fly Ash	86	4.9	9.1

Note: \* indicates the material was not present in the mixture

### 4.2 Moisture-Density Curve

Following the procedure outlined in KT-37, the optimum moisture content was to be determined. This was done by finding the point on a moisture-density curve corresponding to the maximum dry density. The curve outlines the point at which at the “optimum” moisture content, the density is the highest for the mixture. A minimum of 5, 15.5lb samples were obtained for testing. A 6in x 6in Humbolt mold was used for testing. All samples were compacted using 3 lifts with 56 blows of a proctor hammer distributed uniformly over the surface of the layer. KT-37 (KDOT, 2016b) states that when the slump of the specimen is less than 1in, 56 blows of the

hammer is the method to compact the samples. Samples typically started with 5% moisture and 2-3% of moisture were added for each subsequent sample. A polynomial fit curve was applied to the points and the optimum moisture was found. Figure 4-1 shows the moisture-density curve for the Kansas City 100% Cement.

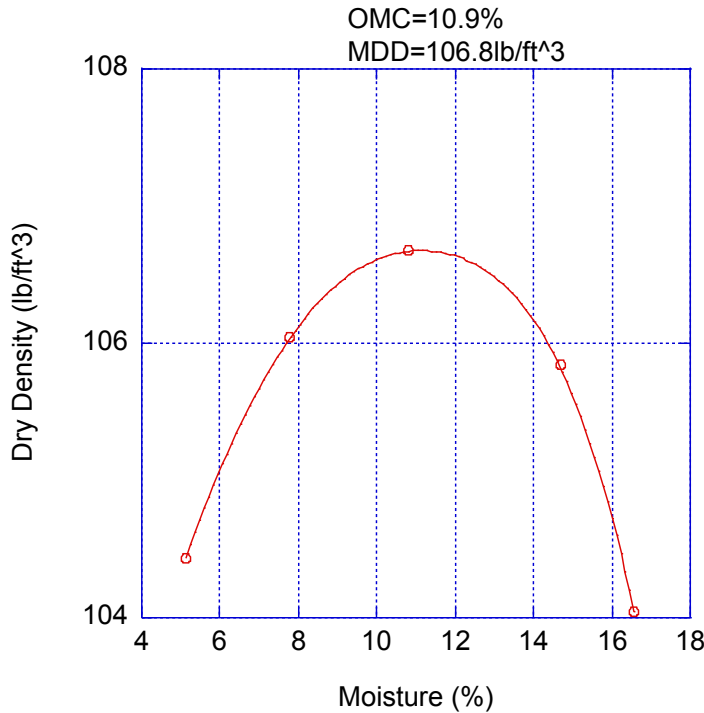


**Figure 4.1 KC 100% Cement Moisture Density Curve**

The moisture density curves tests were conducted for all the RCA and control blends of PCTB. The RCA blends all had negligible differences in optimum moisture, however, the control blends had varying optimum moistures.

### 4.3 Compression Testing

Before batching of cement treated base can begin, the batches must be tested for compressive strength. The KDOT minimum required 7-day unconfined compressive strength (UCS) is 650 psi, and the maximum is 1,600 psi (KDOT, 2015a). Review of PCTB mix designs used by KDOT show an average 7-day UCS of 950 psi. As a result, the design goal was to reach a minimum strength near the KDOT average. Figure 4-2 shows an example of a KDOT blend for treated base. A minimum of 3 samples were prepared for each PCTB mixture. Table 4-2 summarizes the final mix proportions as well as the UCS determined from testing. A Humbolt calibrated cylindrical mold of predetermined volume approximately 6 in. in diameter and 6 in. in

height equipped with a removable base plate was used. With the samples being mixed at optimum moisture, slump was negligible. Due to this, a manual compaction hammer was used to compact each layer with 25 blows being evenly distributed uniformly over the surface of the layer. Three approximately layers of material were placed and compacted in the same manner.

DTMT259		STATE OF KANSAS - DEPARTMENT OF TRANSPORTATION								PAGE: 1
DATE: 01/30/17		TIME: 08:33 AM		LIST OF CEMENT TREATED BASE MIX DESIGNS						
DISTRICT : 1										
CTB MIX #:	1CES220A	E	MATERIAL CODE:		260200011	NAME:		CTB (MODIFIED) LEAN		
% CEMENT/FLY ASH:	5.8	% MOIST:	11.4	EFFECTIVE DATE:	05/01/14	TERMINATION DATE:	01/01/20			
AGGR	NAME	PROD #		PROD NAME		% BLEND				
005010017	AGGR/PCTB(LIMESTONE)	00800977		HAMM QUARRY (044)		100.0				
						0.0				
						0.0				
CEMENT	NAME	PROD #		PROD NAME		% BLEND				
161060100	CEMENT TY1/2 (MH) BULK	00007603		CENTRAL PLAINS (MO)		100.0				
						0.0				
ADDITIVE	NAME	PROD #		PROD NAME		% BLEND				
						0.00				
						0.00				
SIEVE	1.5	1	3/4	1/2	#4	#8	#40	#100	#200	
SINGLE PT.	0.0	2.0	7.0	0.0	54.0	66.0	81.0	0.0	86.0	
TOLERANCE	0.0	2.0	10.0	0.0	10.0	10.0	10.0	0.0	5.0	
TEST GRADATION	0	2	7	23	54	66	81	85	86.3	
COMPRESSIVE STRENGTH	A		B		C		AVG			
	750		732		716		733			
REMARKS:	EMERY-SAPP PUGMILL @ MENOKEN RD., TOPEKA.									

Figure 4.2 KDOT Example PCTB Blend

**Table 4-2: PCTB Blend Design % Binder and Compressive Strength**

PCTB Blend	% Binder	7-Day UCS (psi)	Std. Deviation (psi)
Topeka 100% Cement	7	870	44.5
KC 100% Cement	9	928	85.6
Topeka 50% Cement 50% Fly Ash	10	931	65.0
KC 50% Cement 50% Fly Ash	12	980	88.3
Topeka 35% Cement 65% Fly Ash	14	931	85.0
KC 35% Cement 65% Fly Ash	14	877	3.5

#### 4.4 Cement Treated Base Batching

Materials were prepared in accordance with KTMR-22 before mixtures were batched. All materials were batched in a 2 ft<sup>3</sup> pan mixer using the procedure provided in ASTM C192: Standard Practice for Making and Curing Concrete Test Specimens in the Laboratory (ASTM, 2015b):

1. Place coarse aggregate in mixer;
2. Add approximately half of the mixing water;
3. Start mixer;
4. Add fine aggregate;
5. Add cement;
6. Add remaining half of mixing water;
7. Start timer and mix for 3 minutes with lid open;
8. Stop mixer and let concrete sit still for 3 minutes with lid closed; and
9. Start mixer and mix for additional 2 minutes with lid open;

## **4.5 Preparation of Cement Treated Base Prisms**

Concrete prisms with dimensions of 3 in. x 4 in. x 16 in. were made after batching. As the cement base was mixed with optimum moisture, the mixture was very stiff and rodding or vibrating were not appropriate methods of compaction. Approximately half of the prism height was filled with fresh cement base and compacted with the proctor hammer 25 times. All faces of the prism mold were then struck with a mallet several times before spading the PCTB along the prism edges. This process was repeated after filling the second half of the mold. A wood trowel was used to smooth the exposed face of the prism. The KTMR-22 curing method was used for both the RCA and control samples. KTMR-22 (KDOT, 2015b) outlines KDOT's standard 90-day curing procedure used for samples subjected to freezing and thawing. These samples were placed in a 100% moist room for 67 days. They were then transferred into a ASTM C511 "cement mixing room", room at approximately 50% relative humidity for 21 days before spending two consecutive 24-hour soaking periods in 70°F and 40°F water. To achieve the temperature of 40°F, ice was added to the tank and monitored with a temperature gauge.

## **4.6 ASTM C666 Testing**

Freeze-thaw testing for accelerated cure samples was conducted in accordance with ASTM C666 Procedure B (ASTM, 2015c). A freeze-thaw machine developed by Scientemp Corporation was used to automatically cycle concrete specimens through temperatures specified by ASTM C666. The chamber in this machine has a capacity of 20 concrete prisms. Two of the slots contained control prisms which were used to monitor internal concrete temperatures through thermocouple wires. Test specimens occupied the remaining 18 slots. The freeze-thaw machine was programmed to complete one cycle every three hours. Specimen temperatures were  $40 \pm 3^\circ\text{F}$  at the beginning of each cycle. They were subjected to freezing in air for 110 minutes until they reached  $0 \pm 3^\circ\text{F}$ . The chamber then filled with tempered water, which allowed the samples to thaw.

Mass, resonant frequency, and expansion readings were recorded for all prisms before the beginning of the first freeze-thaw cycle. These values were then recorded in intervals of no more than 36 cycles. Testing continued until samples completed 660 cycles as specified by KTMR-22 (KDOT, KTMR-22: Resistance of Concrete to Rapid Freezing and Thawing, 2015b), or until freeze-thaw deterioration prevented measurements from being taken.

### 4.6.1 Mass Measurements

Mass was recorded using a scale with a capacity of 30kg, which meets ASTM C666 requirements. ASTM C666 requires that the mass of the specimens be no more than 50% of the capacity of the scale. The mass of the specimens ranged from 6 and 8 kg. A towel was used to remove surface water from the prisms in order to maintain consistent conditions when recording mass.

Change in mass was calculated using Equation 1.

$$\text{Change in Mass (\%)} = \left( \frac{m_x - m_o}{m_o} \right) * 100 \quad \text{Equation 1}$$

Where:  $m_x$  = Mass reading at freeze-thaw cycle x (kg.)  
 $m_o$  = Initial mass reading (kg.)

### 4.6.2 Resonant Frequency Measurements

Transverse resonant frequency was obtained using a James E-Meter™ Mk II. The meter is equipped with an impactor and an accelerometer. Figure 4.3 shows the James E-Meter™ Mk II with the accelerometer and impactor.



Figure 4.3 James E-Meter™ Mk II with Accelerometer and Impactor.

The prism transverse resonant frequency was obtained using a modified method of ASTM C215 specified by KTMR-22. Prism dimensions and mass were entered first into the meter. The accelerometer was placed 25 mm away from the end of the prism and then the impactor was used to strike the prism 25 mm from the opposite end. The frequency was then computed by the meter. Equation 2 shows how the transverse frequency values were used to calculate the relative dynamic modulus of elasticity (RDME) of each sample.

$$RDME (\%) = \frac{n_x^2}{n_o^2} * 100 \quad \text{Equation 2}$$

Where:  $n_x$  = Transverse frequency at freeze-thaw cycle x (Hz.)  
 $n_o$  = Initial transverse frequency (Hz.)

Figures 4.4 and 4.5 depict the transverse frequency wave as it propagates through the specimen. The wave is a sinusoidal decay wave and as a specimen deteriorates, the wave amplitude becomes much smaller as shown in Figure 4.5.

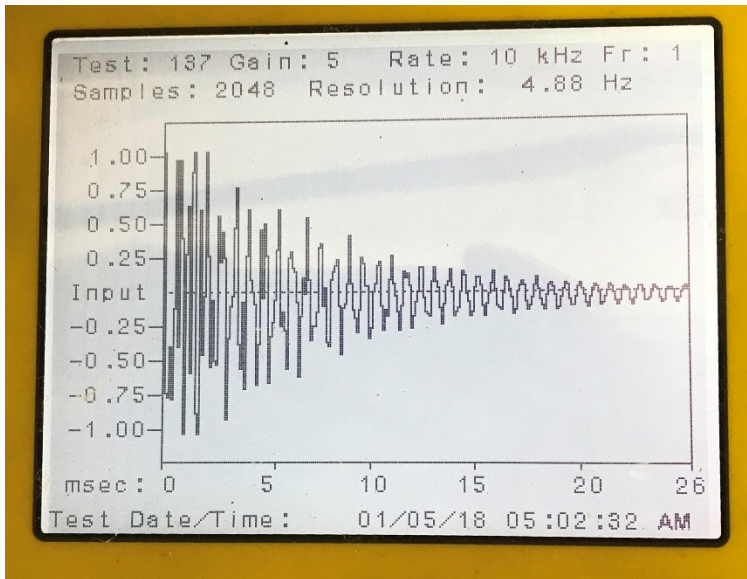


**Figure 4.4 Transverse Frequency Wave of Sample before Testing**

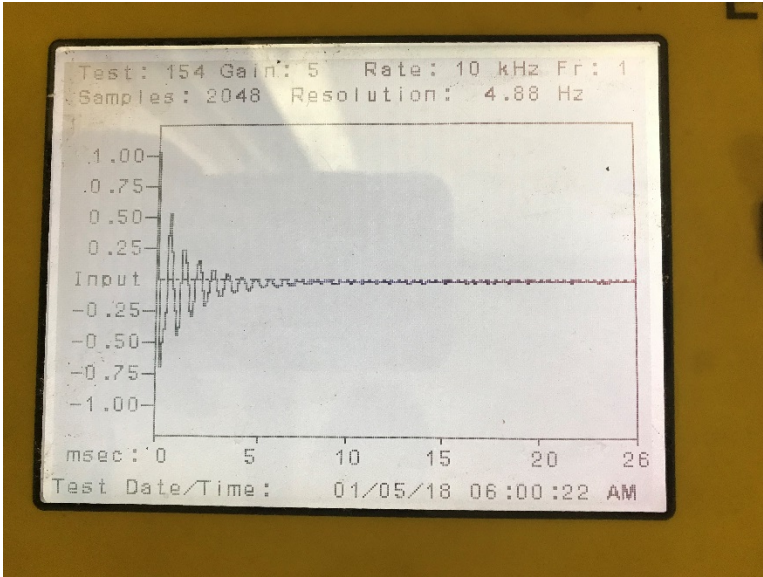


**Figure 4.5 Transverse Frequency Wave of Sample Near Failure**

With the image of the wave having a appearance of those shown in figures 4.4 and 4.5, the data is then accepted and an image that shows the transverse frequency will appear and the largest frequency is the value that is recorded. Figure 4.6 shows a sample that had been tested and the frequency that was recorded.

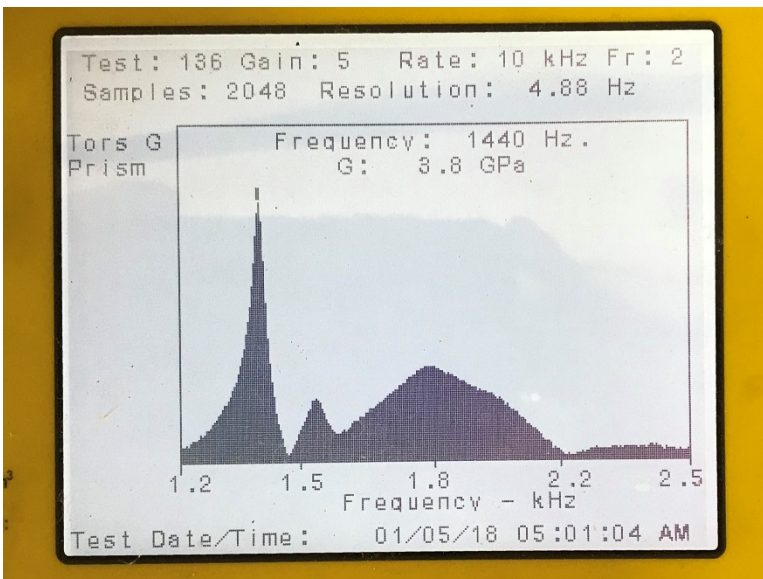


**Figure 4.6 Typical Sample Transverse Frequency**

### 4.6.3 Expansion Measurements

To measure length change, or expansion, of the prisms, steel gauge studs were installed in both ends of the prisms during mixing. The molds that were used allowed for the studs to be set in a constant place during curing. The initial length of each prism was measured prior to the first freeze-thaw cycle. The difference in length between each prism and a reference bar were compared by placing the reference bar in a length comparator equipped with a digital indicator.

The indicator was set to zero in order to establish a reference point from which the length of the prism could be measured. The reference bar was then removed and replaced by the prism. The precision of the digital indicator was to the 0.00001 in. The change in length was monitored continuously throughout testing. Length change was calculated using Equation 3.

$$\text{Length change (\%)} = \left( \frac{l_x - l_o}{l_i} \right) * 100 \quad \text{Equation 3}$$

Where:  $l_x$  = Indicator reading at freeze-thaw cycle x (in.)  
 $l_o$  = Initial indicator reading (in.)  
 $l_i$  = Initial prism length (in.)

## Chapter 5 - D-Cracked RCA Cement Treated Base Study Results

Mass change, RDME, and length change were measured for each samples until 660 freeze-thaw cycles or until excessive deterioration prevented recording of such measurements. Due to the weakened nature of D-cracked aggregate, the samples did not reach the 660 cycle maximum specified by KDOT. This chapter provides a summary and examples of the ASTM C666 results for the D-cracked RCA portion of this study. Representations of mass change, RDME, and length change during testing can be found for each blend of PCTB in Appendix A.

### 5.1 Change in Mass

A summary of change in mass for all samples at their terminal freeze-thaw cycle is shown in Table 5-1. In the column titled PCTB Blend, the names Topeka and KC denote the aggregate source. The percentages denote the blend of the binder within the PCTB. For example, Topeka 50%-Cement 50%-Fly Ash means that the RCA source is from Topeka, and of the total binder percentage, 50% is cement and 50% is fly ash.

**Table 5-1: Summary of D-Cracked RCA Mass Change Results**

PCTB Blend	Average Final Mass Change (%)	Std. Dev. (%)
Topeka 100%-Cement	0.70	0.4
Topeka 50%-Cement 50%-Fly Ash	10.7	6.5
Topeka 35%-Cement 65% Fly Ash	6.64	8.4
Kansas City 100%-Cement	6.71	4.0
Kansas City 50%-Cement 50%-Fly Ash	15.6	5.1
Kansas City 35%-Cement 65%-Fly Ash	12.8	6.1

### 5.2 Relative Dynamic Modulus of Elasticity

The dynamic modulus of elasticity is the proportion of stress to strain when the stress is least under dynamic loads. It can be measured by means of longitudinal vibration or flexural

vibration. It reflects the elasticity performance of material, similarly to the initial tangential modulus under static loads. The loss of the dynamic modulus of elasticity with freeze-thaw cycles means the loss of the elasticity performance (Shang & Yi, 2013). Table 5-2 summarizes the results for the RDME.

**Table 5-2: Summary of D-Cracked RCA RDME Results**

PCTB Blend	Average Final RDME (%)	Std. Dev. (%)	Average Final Cycle	Std. Dev.
Topeka 100%-Cement	52.3	6.7	111	23
Topeka 50%-Cement 50%-Fly Ash	44.8	19.1	200	44
Topeka 35%-Cement 65% Fly Ash	45.8	11.6	285	10
Kansas City 100%-Cement	43.6	17.0	35	7
Kansas City 50%-Cement 50%-Fly Ash	51.2	8.5	169	43
Kansas City 35%-Cement 65%-Fly Ash	50.9	8.1	214	12

### 5.3 Expansion

Measurement of length change permits assessment of the potential for volumetric expansion or contraction of mortar or concrete due to various causes other than applied force or temperature change. Table 5-3 summarizes the results for the expansion.

**Table 5-3: Summary of D-Cracked RCA Length Change Results**

PCTB Blend	Average Final Expansion (%)	Std. Dev. (%)
Topeka 100%-Cement	0.15	0.066
Topeka 50%-Cement 50%-Fly Ash	0.28	0.55
Topeka 35%-Cement 65% Fly Ash	0.17	0.091
Kansas City 100%-Cement	0.39	0.28
Kansas City 50%-Cement 50%-Fly Ash	0.36	0.20
Kansas City 35%-Cement 65%-Fly Ash	0.08	0.048

It should be noted that the results for the average final expansion may not be completely representative of the expansion behavior of the PCTB with RCA. During testing, the largest portion of mass loss occurs on the ends of the prism. With the excessive mass loss, the length change studs will fall out of the specimens and cannot be replaced. The blends with the 35% cement and 65% fly ash saw less stud loss than the two other blends with less binder. With the expansion measurement being an optional test within ASTM C666 (ASTM, 2015c), it is possible to ignore the expansion and solely test based on mass change and RDME.

## Chapter 6 - Control Portland Cement Treated Base Results

To create the control samples, a blend of coarse aggregate and fine aggregate was determined based on the washed sieve analysis of both the RCA and virgin aggregates. Both curves were plotted on the same graph and the blend that best fit the curve was used as the control blend. Figure 6-1 shows the blend curve for the Topeka control samples and Figure 6-2 shows the curve for the KC control samples.

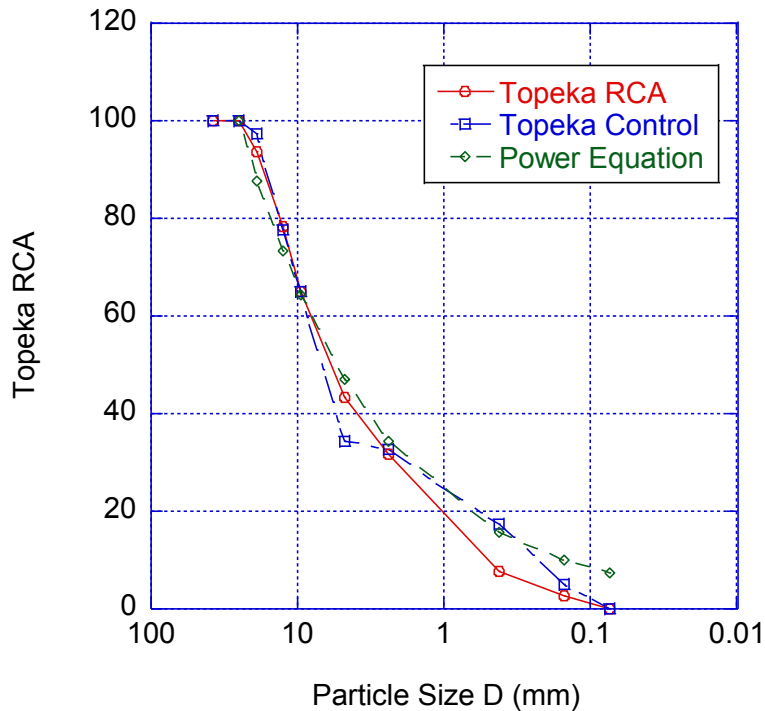


**Figure 6.1: Topeka Control Blend Curve**

The power equation, in Equation 4, is the 0.45 Power Maximum Density Curve equation.

$$P = \left(\frac{d}{D}\right)^{0.45} \quad \text{Equation 4}$$

Where:

- $P =$  % finer than the sieve
- $d =$  Aggregate size being considered
- $D =$  Maximum aggregate size to be used

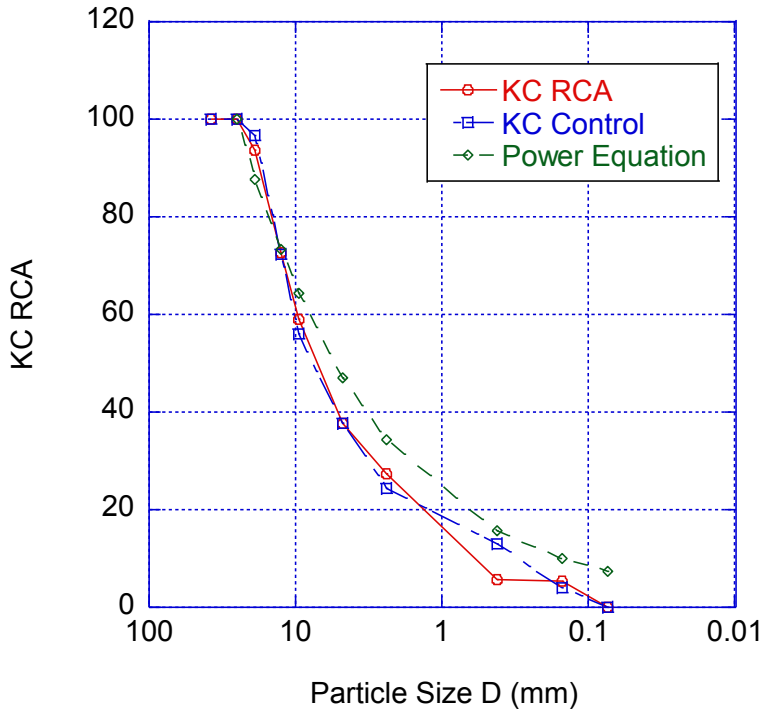


**Figure 6.2: KC Control Blend Curve**

The mix proportion for the Topeka control samples was 52% coarse aggregate and 48% fine aggregate. The mix proportion for the KC control samples was 65% coarse aggregate and 35% fine aggregate.

Following the same testing and mixing procedures as the RCA PCTB, the compressive strength of the control samples was determined. The objective was to have the compressive strength of the control samples similar to that of the RCA samples. The results were close but not exactly the same. It was expected that the strength would be greater at lower percentages of binder, and Table 6-1 shows that. The control samples all had either the same or lower percentages of binder.

**Table 6-1: Average UCS of Control Samples**

PCTB Blend	% Binder	7-Day UCS (psi)	Std. Deviation (psi)
Topeka 100% Cement	7	924	24.5
KC 100% Cement	7	1017	48.5
Topeka 50% Cement 50% Fly Ash	9	1155	42.5
KC 50% Cement 50% Fly Ash	9	940	10
Topeka 35% Cement 65% Fly Ash	11	1087	25.5
KC 35% Cement 65% Fly Ash	11	1080	55

Exactly as the D-cracked RCA in Chapter 5, Mass change, RDME, and length change were measured for each control sample until 660 freeze-thaw cycles or until excessive deterioration prevented recording of such measurements. Similarly to the RCA treated base samples, the control samples did not reach the maximum 660 cycles specified by KDOT. Only the 100%-Cement and 50%-Cement 50%-Fly Ash samples were tested. Time constraints resulted in the 35%-Cement 65%-Fly Ash sample testing to be postponed. This chapter provides a summary and examples of the ASTM C666 results for the control portion of this study. Representations of mass change, RDME, and length change during testing can be found for each blend of control cement treated base in Appendix A.

## 6.1 Change in Mass

A summary of change in mass for all samples at their terminal freeze-thaw cycle is shown in Table 6-1.

**Table 6-2: Summary of Control Mass Change Results**

Sample Set	Average Final Mass Change (%)	Std. Dev. (%)
Topeka Control 100-Cement	0.3	0.22
Topeka Control 50%-Cement 50%-Fly Ash	4.3	0.07
Kansas City Control 100%-Cement	0.5	0.43
Kansas City Control 50%-Cement 50%-Fly Ash	5.0	1.3

## 6.2 Relative Dynamic Modulus of Elasticity

**Table 6-3: Summary of Control RDME Results**

Sample Set	Average Final RDME (%)	Std. Dev. (%)	Final Cycle	Std. Dev.
Topeka Control 100-Cement	38.0	16.7	40	6
Topeka Control 50%-Cement 50%-Fly Ash	56.5	1.3	196	18
Kansas City Control 100%-Cement	41.1	18.7	44	6
Kansas City Control 50%-Cement 50%-Fly Ash	55.3	2.6	166	17

### 6.3 Expansion

**Table 6-4: Summary of Control Length Change Results**

Sample Set	Average Final Expansion (%)	Std. Dev. (%)
Topeka Control 100%-Cement	0.06	0.003
Topeka Control 50%-Cement 50%-Fly Ash	0.02	0.009
Kansas City Control 100%-Cement	0.05	0.062
Kansas City Control 50%-Cement 50%-Fly Ash	0.03	0.004

## Chapter 7 - Analysis and Discussion

### 7.1 D-Cracked RCA Cement Treated Base

As anticipated, the D-cracked PCTB did not reach the 660 cycle mark specified in KTMR-22. Unlike concrete, PCTB is a very porous material and as a result allows for excess water to penetrate into the sample, accelerating the deterioration during freeze-thaw conditions. Figure 7.1 shows the average cycle where the samples fell below the 60% RDME.

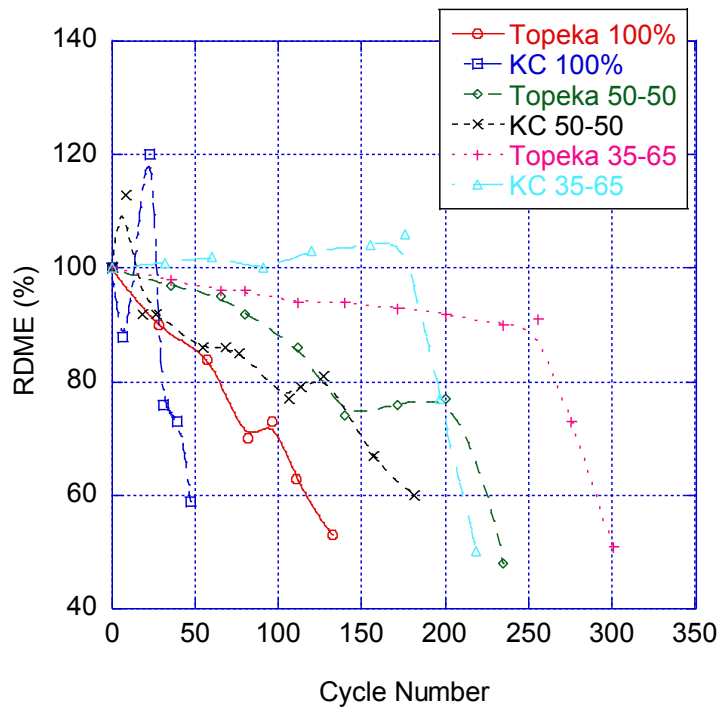


**Figure 7.1 Average RCA RDME Trend During Study**

From Figure 7-1, it is shown that an increase in binder content (i.e. cement and fly ash), results in an increase in durability of the samples. It is theorized that this occurs because with a higher portion of fines in the PCTB, there are less voids in the samples which in turn limits the deterioration from freeze-thaw. It is also shown that the composition of the pavement plays a part in the durability in the samples as the Topeka and KC samples had differing performance. The KC samples with 100% cement displayed an unexpected behavior at the beginning of the testing between 10 and 25 cycles. There is a rapid increase in the RDME over the course of a few cycles. A possibility of this behavior is initial cracks caused by the freeze-thaw cycling allows

excess water to penetrate the samples but not escape. This additional mass can cause the RDME to increase as the sample becomes more dense, which allows for the wave from the impact of the hammer to propagate faster through the sample. This behavior can be seen in Appendix B showing the change in RDME over the course of the testing for each sample. The behavior is not present in the Topeka samples, but another behavior is noticed. The 35%-Cement 65%-Fly Ash samples appear to have a “yield point.” This is shown by the steady linear performance until it reaches a specific number of cycles, after that, the specimens begin to rapidly deteriorate. Figure 7-2 depicts the mass change during the course of the study. As noted before, an increase in mass is seen in the beginning of the freeze-thaw cycling. As the samples continue to degrade, there is a period of increased RDME shortly before the samples will rapidly degrade and fail. While it is not as prevalent in the 35% Cement 65% Fly Ash blend, there is a noticeable change in the two other blends for the Topeka samples.

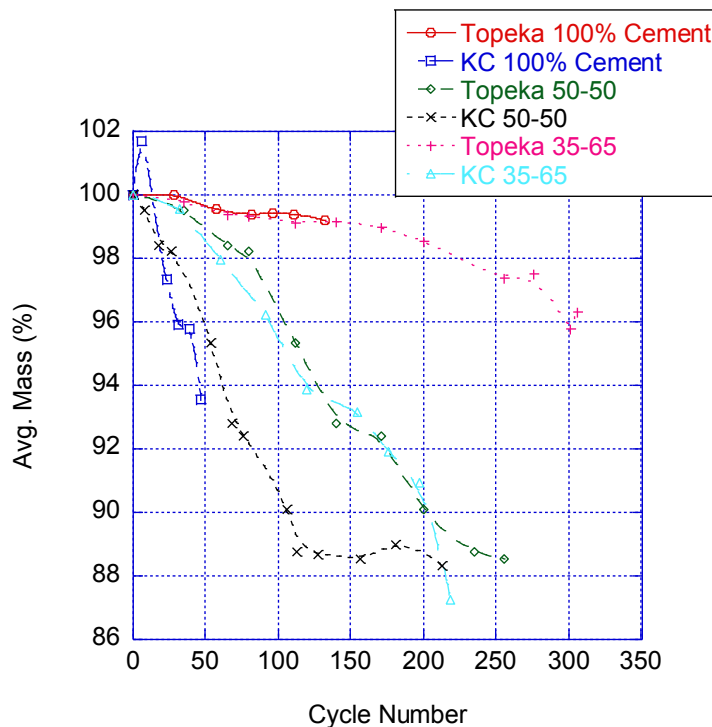


**Figure 7.2 RCA Mass Change During Study**

When comparing the 100% cement samples, the Topeka greatly out-performs the KC samples. The average cycle at failure for the Topeka samples is 111 while the KC is 35. It is not clear as to why the Topeka samples lasted over 3 times as long as the KC samples. The mass loss of the Topeka samples is almost negligible while the KC samples lost approximately 7% of the

mass. The behavior of the Topeka samples is interesting as it was assumed that the 100% cement samples would have the largest mass loss. The expansion of the Topeka samples is also less than that of the KC samples.

Comparing the 50% cement 50% fly ash samples, the Topeka once again out-performed the KC samples. The average cycle at failure for the Topeka samples is 200 while the KC is 169. The convergence of the performance is likely attributed to the increase binder content of the samples.

The average final cycle for the Topeka and KC 35% cement 65% fly ash samples are 285 and 214 respectively. Just as the previous samples, it is shown that an increase in total binder content increases the freeze-thaw durability of the samples. Looking at Figure 7.1, it is shown that the Topeka and KC exhibit a similar behavior. There is a linear portion of change in the RDME followed by a sharp decrease until failure. It is assumed that the higher binder percentages allows for better performance until it reaches a level of deterioration, which at that point, the samples degrade rapidly.

## **7.2 Control Portland Cement Treated Base**

Similarly to the RCA, the control samples did not meet the 660 cycle criteria specified by KDOT. However, besides the Topeka 100%, the control samples had durability comparable to those of the PCTB. The KC 100% cement control samples performed better than the RCA samples, but the 50-50 blends for the control samples underperformed compared to the RCA. The control samples however, had less binder and failed an average of 3.5 cycles sooner than the RCA samples. The control samples had very similar performance compared to each other. This is expected as the coarse and fine aggregates are the same. Figure 7.3 shows the average RDME trend over the life of the control samples. Figure 7.4 shows a comparison of the KC control and RCA samples. The RCA samples have an unpredictable behavior during freeze-thaw testing, whereas the control samples follow a linear trend. Both however, have similar durability in terms of the RDME limit. Appendix E has comparisons of the PCTB with RCA and the control specimens with error bars to show that the control samples have less variability in behavior and performance than those of the RCA.

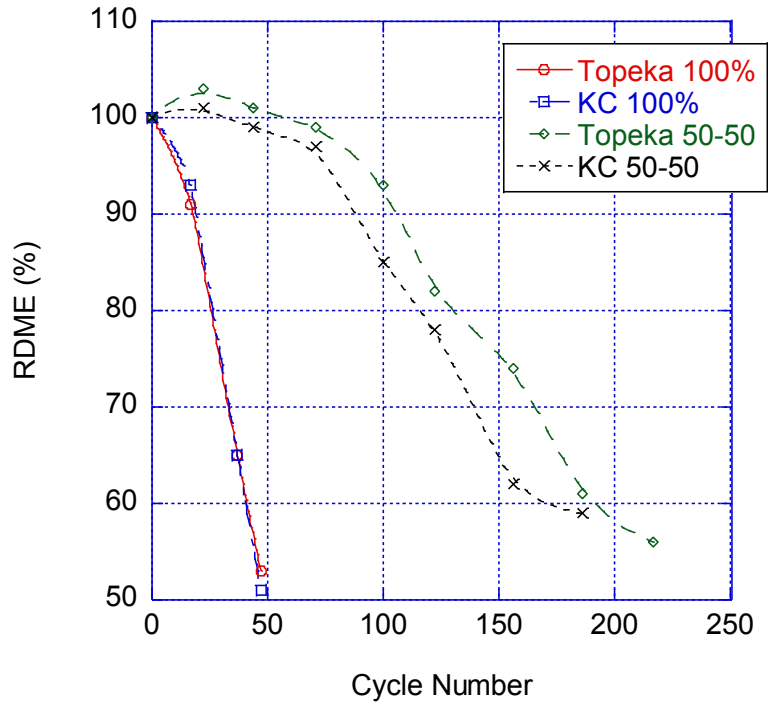


**Figure 7.3 Control Sample RDME Trend During Study**

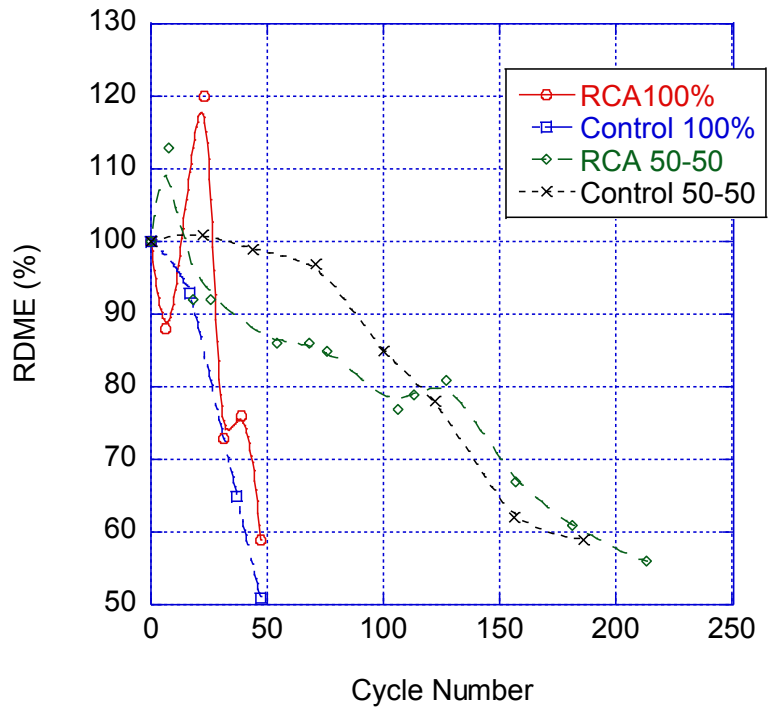


**Figure 7.4 KC RCA and Control RDME Trend Comparison**

## **Chapter 8 - Conclusions**

Increasing the binder content yielded in higher durability results when compared to those of lower binder contents. At lower binder contents, the composition of the aggregates in the RCA seem to be a controlling factor in durability. When the binder content increases, the role of the coarse aggregate seems to be less of a controlling factor since the samples are less porous. As predicted, none of the sample sets reached the 660 cycles for testing. With the mixing being conducted at optimum moisture content, the result from the mixing is a more porous material than a normal concrete pavement would be.

With the exception of the Topeka 100% cement samples, the control samples for the other sets had very similar durability. Testing on the 35% cement and 65% fly ash for both Topeka and KC control samples need to be conducted to see if the same trend of comparable durability continues. This correlation between the D-cracked RCA and control samples is promising as D-cracked RCA was expected to perform more poorly than the control samples. This shows that total binder percentage is the main controlling factor in performance of PCTB in freeze-thaw conditions.

### **8.1 Recommendations for Future Research**

Freeze-thaw results for the 35% cement 65% fly ash have yet to be completed. These results can verify or reject the close correlation between the RCA and control samples. Additional blends of cement and fly ash such as 75% cement 25% fly ash or 25% cement and 75% fly ash should be created to determine an optimum blend of cement and fly ash for freeze-thaw performance of PCTB containing RCA. Dry sieving over a #18 (1.00mm) sieve to remove excess fines before testing for optimum moisture and compressive strength could be a method to achieve a more homogeneous gradation for the RCA, as the gradation can heavily vary due to the crushing, transportation, storage of the RCA as well as settlement of fines.

Currently, KDOT does not have any specifications for the freeze-thaw durability of PCTB. With performance not meeting the 660 cycles for even the control samples, as well as large mass loss for the RCA samples, a shorter cycle criteria and a mass loss criteria should be developed to more accurately test the durability of PCTB.

## References

- ACPA. (2009). *Recycling Concrete Pavements*.
- Ashraf, W., Glinicki, M. A., & Olek, J. (2018). *Probabilistic Approach for Composition Selection of Freeze–Thaw Resistant Ordinary Portland Cement Concrete*. Transportation Research Board 97th Annual Meeting Transportation Research Board.
- ASTM. (2013). Standard Test Method for Soundness of Aggregates by Use of Sodium Sulfate or Magnesium Sulfate. *ASTM International*.
- ASTM. (2014). ASTM C131: Standard Test Method for Resistance to Degradation of Small-Size Coarse Aggregate by Abrasion and Impact in the Los Angeles Machine. *ASTM International*.
- ASTM. (2015a). ASTM C128: Standard Test Method for Density, Relative Density (Specific Gravity), and Absorption of Fine Aggregate. *ASTM International*.
- ASTM. (2015b). ASTM C192: Standard Practice for Making and Curing Concrete Test Specimens in the Laboratory. *ASTM International*.
- ASTM. (2015c). ASTM C666: Standard Test Method for Resistance of Concrete to Rapid Freezing and Thawing. *ASTM International*.
- ASTM. (2015d). Standard Test Method for Relative Density (Specific Gravity) and Absorption of Coarse Aggregate. *ASTM International*.
- E701, A. C. (2016). *E-1(16) Aggregates for Concrete*. American Concrete Institute.
- Embacher, R. A., & Snyder, M. B. (2003). *Refinement and Validation of the Hydraulic Fracture Test*. St. Paul: Minnesota Department of Transportation.
- FHWA. (2006). *Freeze-Thaw Resistance of Concrete With Marginal Air Content*. U.S. Department of Transportation.
- Fredlund, D., & Rahardjo, H. (1993). *Soil Mechanics for Unsaturated Soils*. Danvers: John Wiley & Sons.
- Jonsson, J. A., & Olek, J. (2004). Effect of Temperature-Match-Curing on Freeze-Thaw and Scaling Resistance of High-Strength Concrete. *Cement, Concrete, and Aggregates*.
- KDOT. (1999). *KTMR-21 Soundness and Modified Soundness of Aggregates by Freezing and Thawing*. Topeka: Kansas Department of Transportation.
- KDOT. (1999). *KTMR-21: Soundness & Modified Soundness of Aggregates by Freezing and Thawing*. Topeka: Kansas Department of Transportation.
- KDOT. (2015a). *306 - Cement Treated Base*. Topeka: Kansas Department of Transportation.

- KDOT. (2015b). *KTMR-22: Resitance of Concrete to Rapid Freezing and Thawing. KDOT Standard Specifications for State Road and Bridge Construction*. Topeka, Kansas.
- KDOT. (2016a). *KT-2 Sieve Analysis of Aggregates*. Topeka: Kansas Department of Transportation.
- KDOT. (2016b). *KT-37: Making, Curing and Testing of Cement Treated and Unbound Bases*. Topeka: Kansas Department of Transportation.
- Lee, M.-G. (2007). *Preliminary Study for Strength and Freeze-Thaw Durability of Microwave- and Steam-Cured Concrete*. *Journal of Materials in Engineering*.
- MDOT. (2015). *MTM 115*.
- O'Doherty, J. (1987). D-Cracking of Concrete Pavements. *Materials and Technology Engineering and Science*.
- ODOT. (2013). Aggregates. *Construction and Material Specifications*, 717-718.
- Oikonomou, N. D. (2005). Recycled concrete aggregates. *Cement and Concrete Composites*, 315-318.
- Pigeon, M., & Pleau, R. (1995). *Durability of Concrete in Cold Climates*. London and New York: Taylor and Francis.
- Pigeon, M., Pleau, R., & Aitcin, P.-C. (1986). *Freeze-Thaw Durability of Concrete With and Without Silica Fume in ASTM C 666 (Procedure A) Test Method: Internal Cracking Versus Scaling*. CCAGDP.
- Powers, T. C. (1945). *A Working Hypothesis for Further Sudies of Frost resistance of Concrete*. *ACI Journal*.
- Powers, T. C. (1949). *The Air Requirement of Frost Resistant Concrete*. Research and Developments Laboratories of the Portland Cement Association.
- Powers, T. C., & Helmuth, R. A. (1953). *Theory of Volume Changes in Hardened Portland Cement Paste During Freezing*. Research and Developments Laboratories of the Portland Cement Association.
- Ranaivomanana, H., Verdier, J., Sellier, A., & Bourbon, X. (2011). Toward a better comprehension and modeling of hysteresis cycles in the water sorption–desorption process for cement based materials. *Cement and Concrete Research* 41, 817-827.
- Rao, A., Jha, K. N., & Misra, S. (2007). Use of aggregates from recycled construction and demolition waste in concrete. *Resour.Conserv.Recycling*, 71-81.
- Schwartz, D. (1987). *D-Cracking of Concrete Pavements*. Washington, DC: Transportation Research Board.

- Shang, H.-S., & Yi, T.-H. (2013). Freeze-Thaw Durability of Air-Entrained Concrete. *The Scientific World Journal*.
- Silva, R. V., Brito, J. d., & Dhir, R. K. (2016). Establishing a relationship between modulus of elasticity and compressive strength of recycled aggregate concrete. *J.Clean.Prod*, 112 2171-2186.
- Thompson, S. R., Olsen, M. P., & Dempsey, B. J. (1980). *D-Cracking in Portland Cement Concrete Pavements*. Illinois Cooperative Highway and Transportation Research Program.
- Verian, K. P., Whiting, N. M., Olek, J., Jain, J., & Snyder, M. B. (2013). *Using recycled concrete aggregate in concrete pavements to reduce materials cost*.
- Whitehurst, E. A. (1980). D-cracking and Aggregate Size.
- Woodhouse, T. (2005). *Multi-State Coarse Aggregate Freeze-Thaw Comparison*. Lansing: Michigan Department of Transportation.
- Wu, Z., Shi, C., Gao, P., Wang, D., & Cao, Z. (2015). *Effects of Deicing Salts on the Scaling Resistance of Concrete*.

## Appendix A - D-Cracked RCA Moisture Density Curves

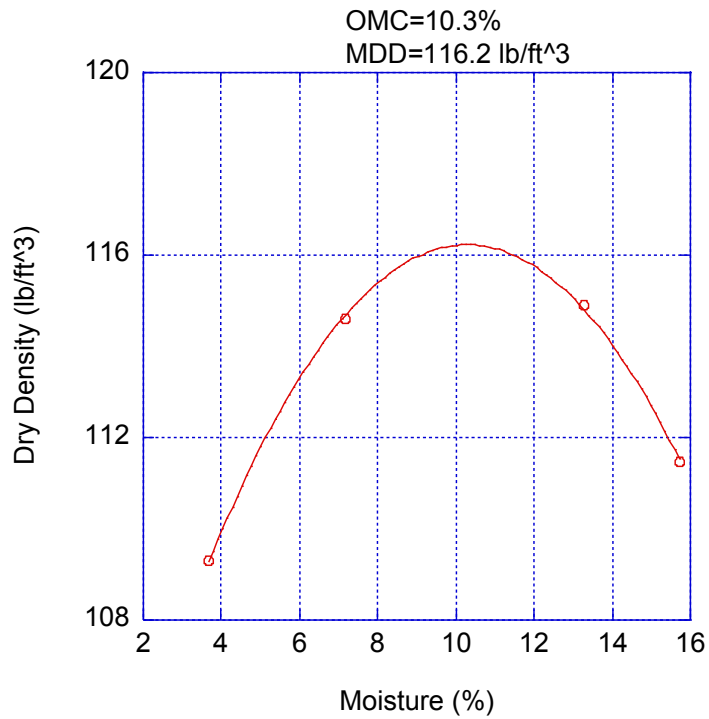
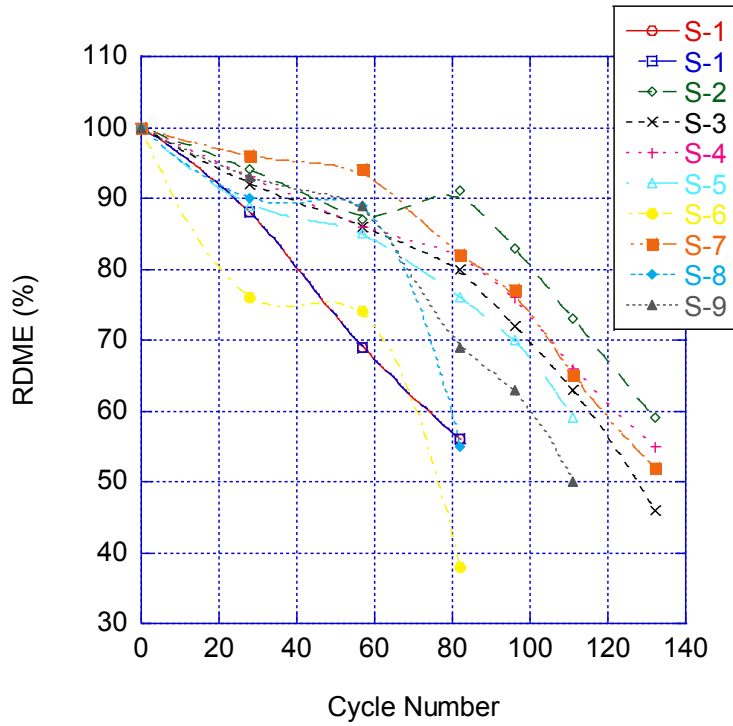
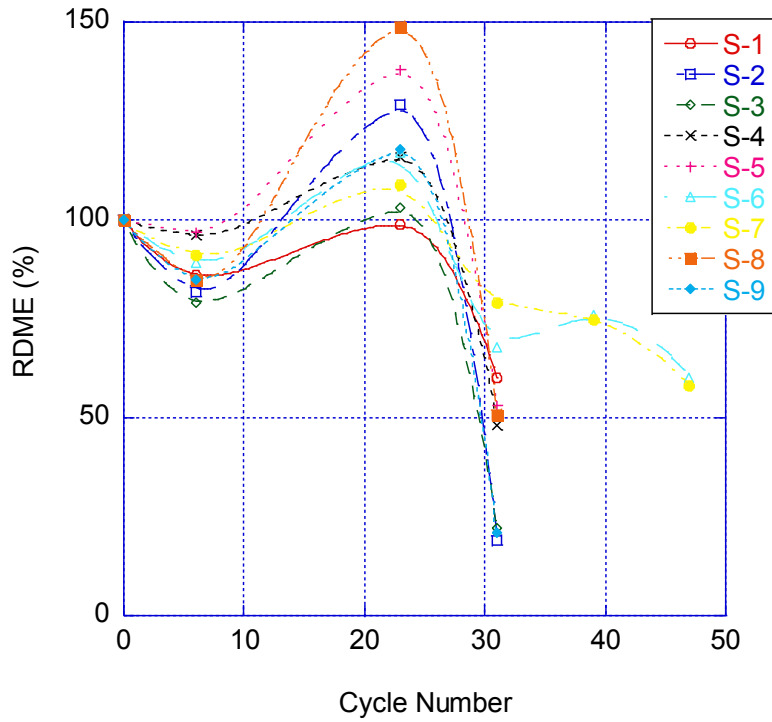


Figure A.1 Topeka 100% Cement Moisture Density Curve

## Appendix B - D-Cracked RCA ASTM C666 Results



**Figure B.1 Topeka 100% Cement Freeze-Thaw Trend**



**Figure B.2 KC 100% Cement Freeze-Thaw Trend**

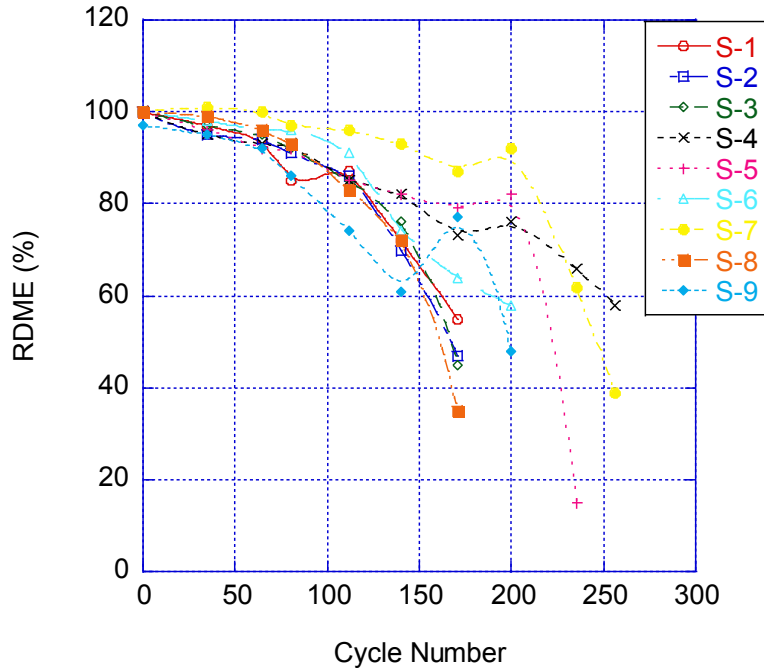


Figure B.3 Topeka 50% Cement 50% Fly Ash Freeze-Thaw Trend

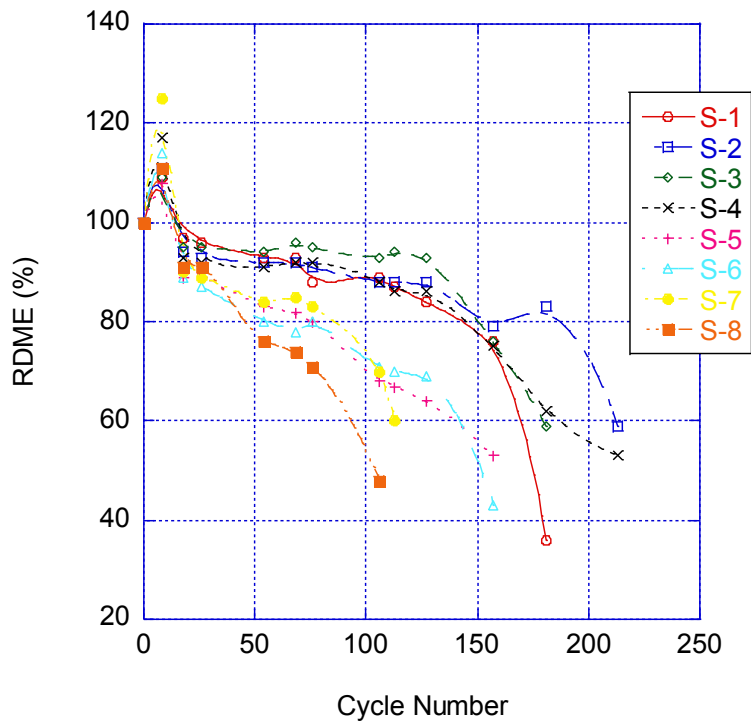
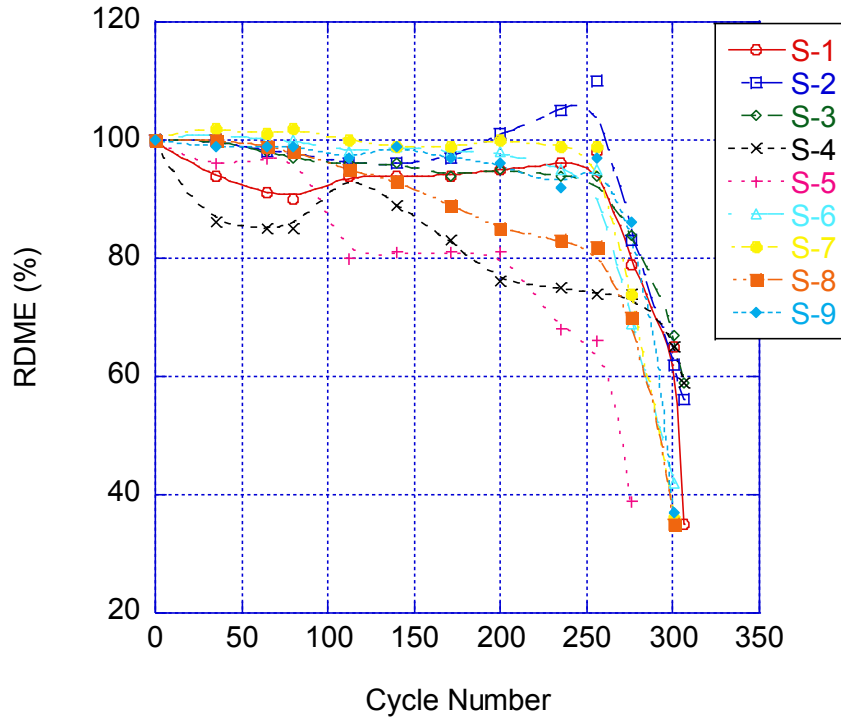
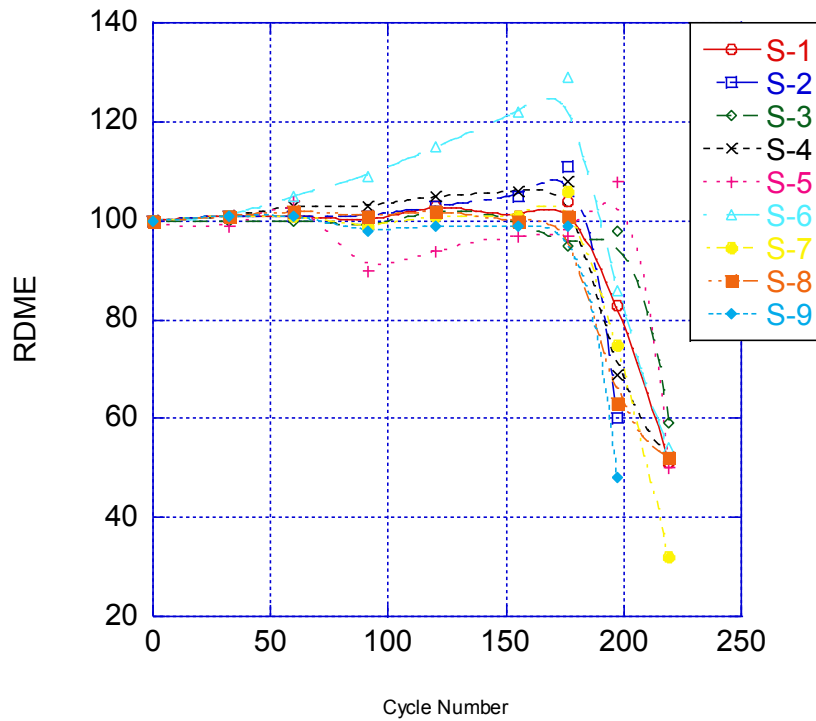


Figure B.4 KC 50% Cement 50% Fly Ash Freeze-Thaw Trend



**Figure B.5 Topeka 35% Cement 65% Fly Ash Freeze-Thaw Trend**



**Figure B.6 KC 35% Cement 65% Fly Ash Freeze-Thaw Trend**

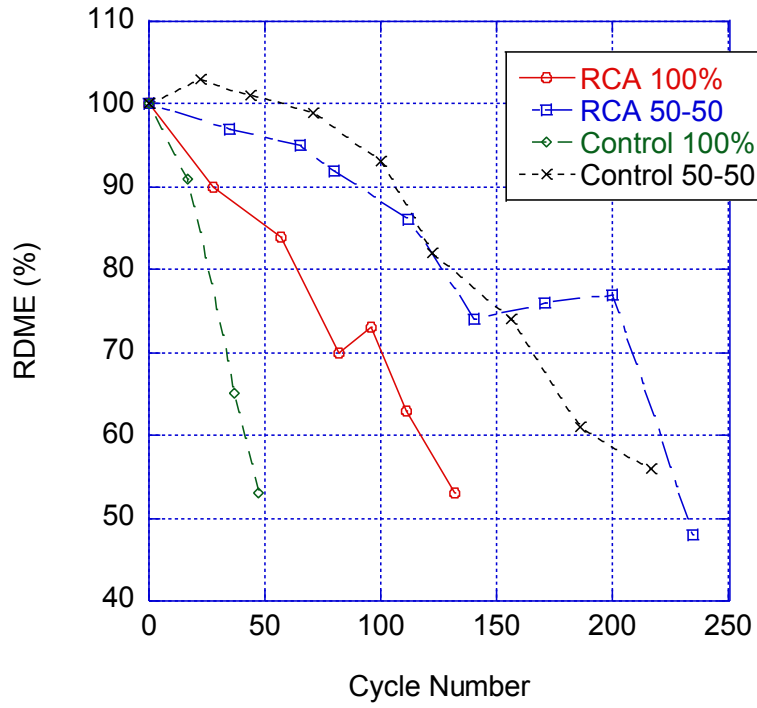


**Figure B.7 Topeka RCA and Control Comparison**

## Appendix C - Control Moisture Density Curves

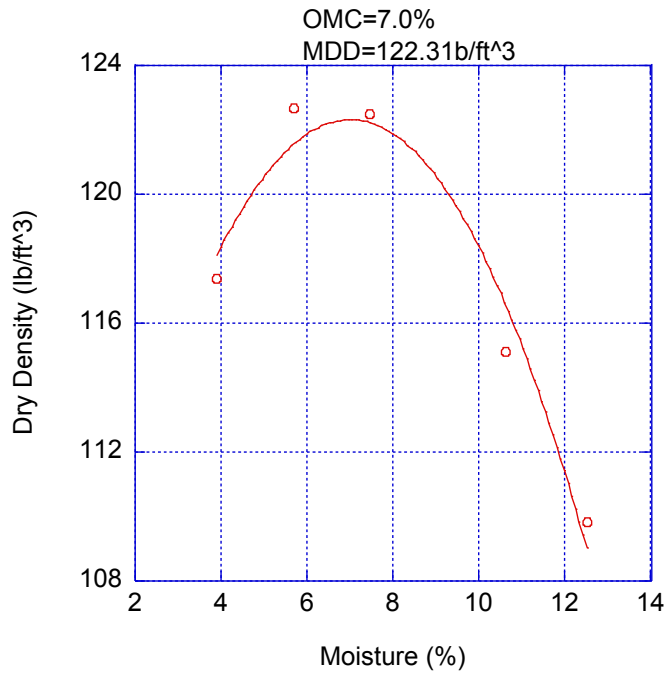


Figure C.1 Topeka Control 100% Cement Moisture Density Curve

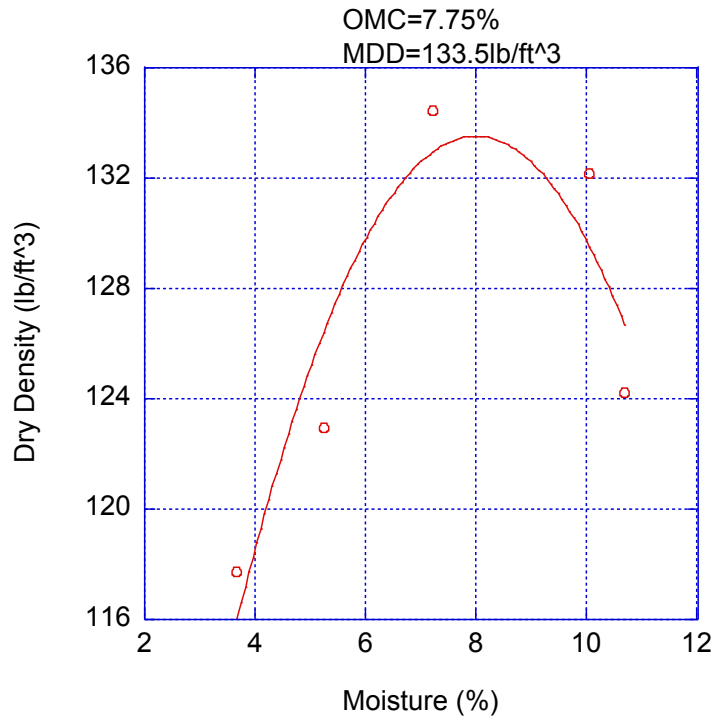
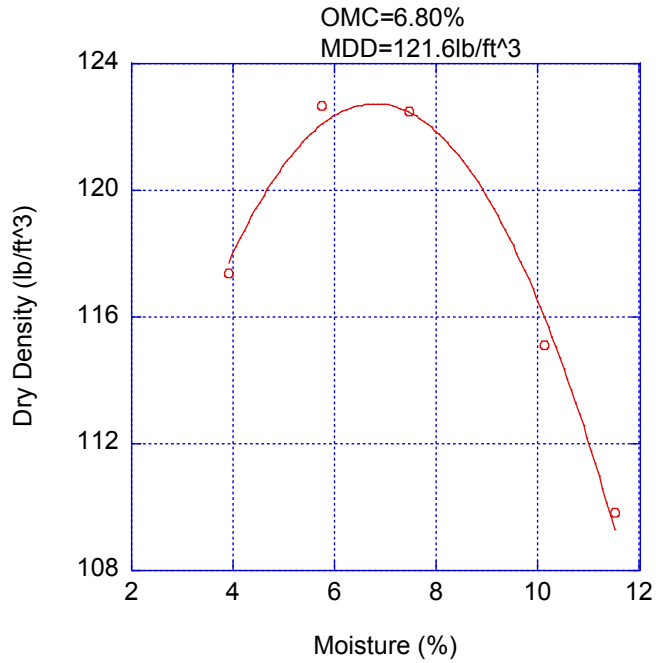
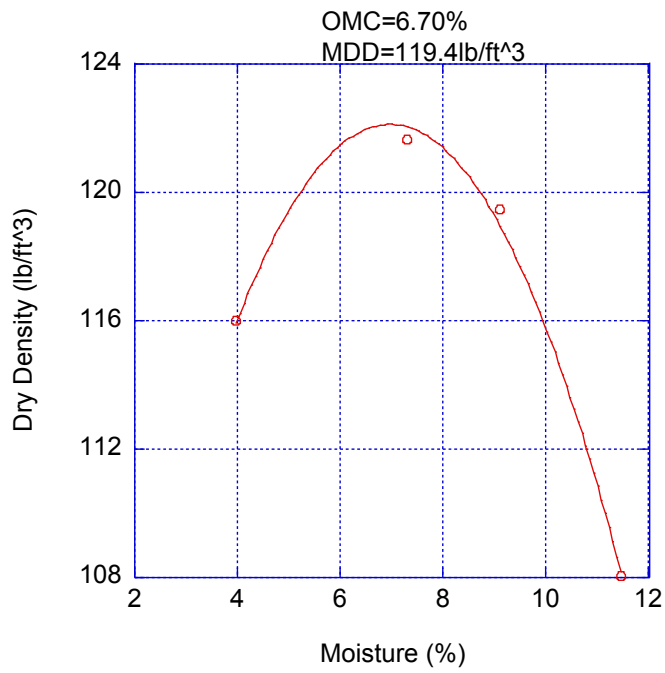


Figure C.2 KC Control 100% Moisture Density Curve



**Figure C.3 Topeka Control 50-50 Moisture Density Curve**



**Figure C.4 KC Control 50-50 Moisture Density Curve**

## Appendix D - Control ASTM C666 Results

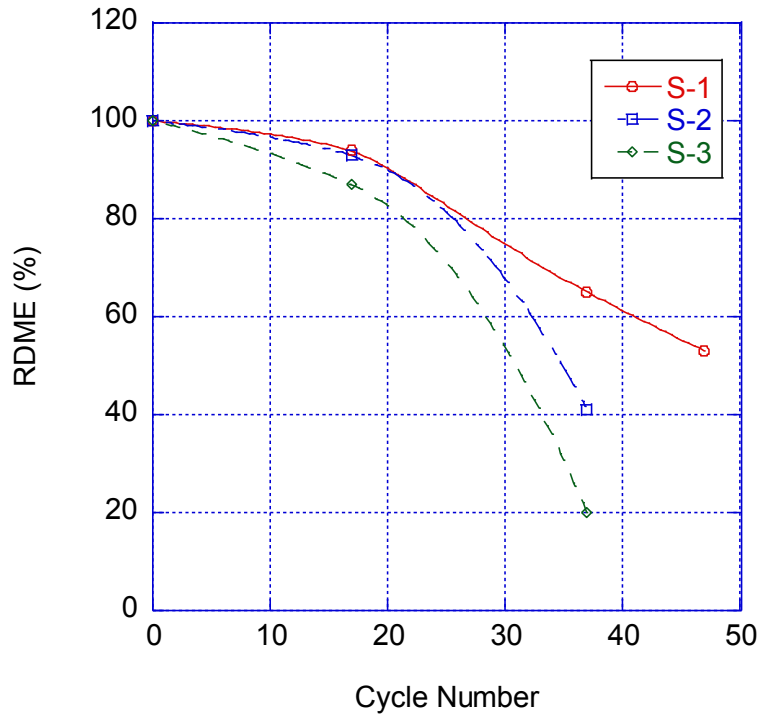


Figure D.1 Topeka Control 100% Cement Freeze-Thaw Trend

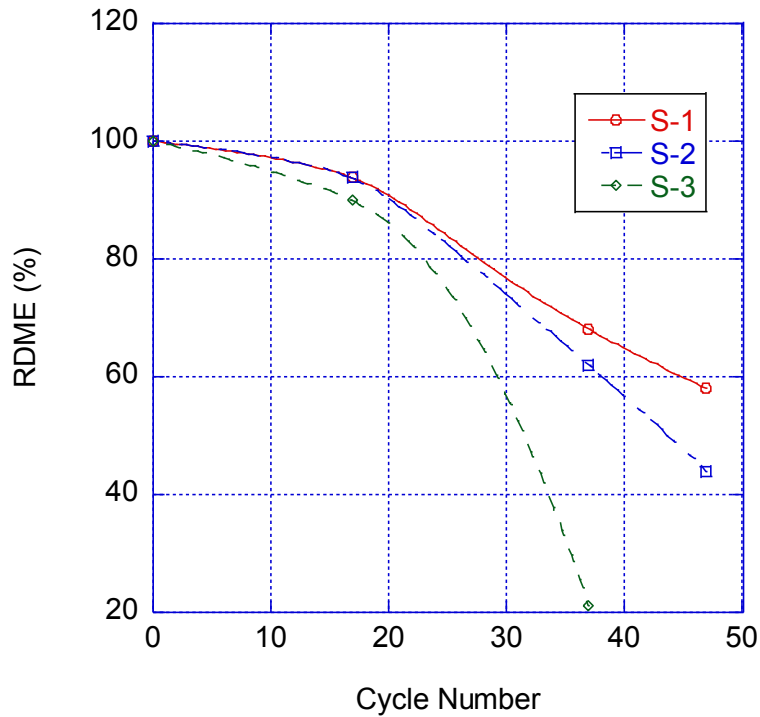
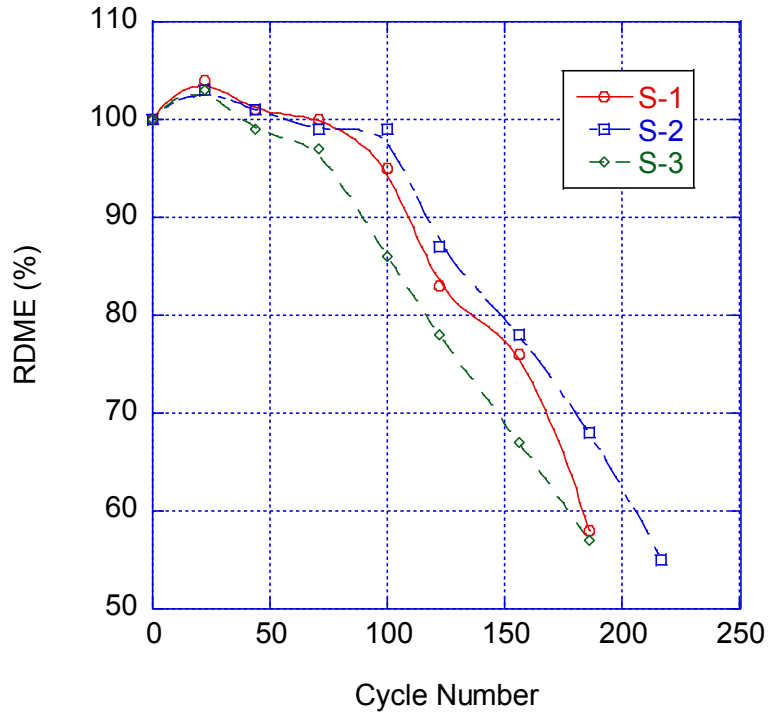
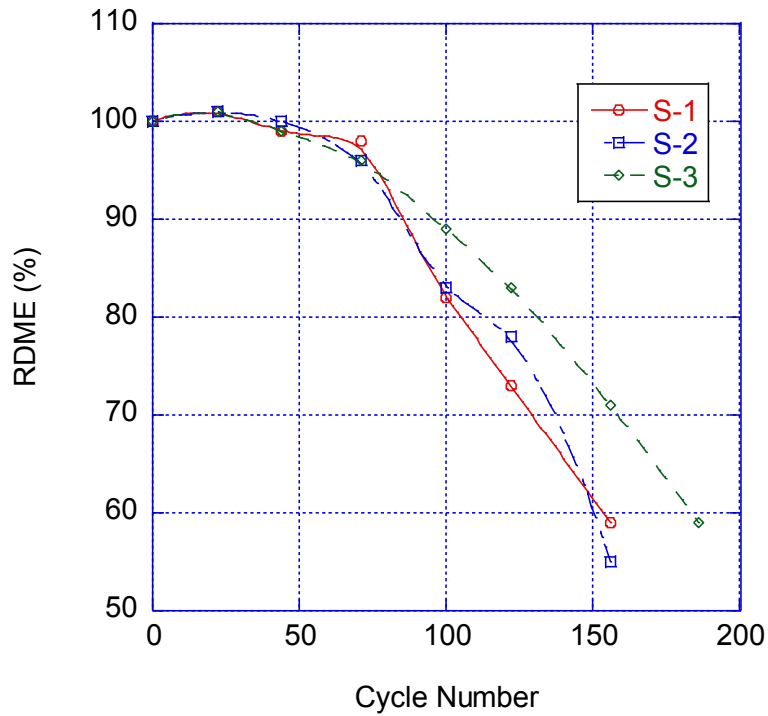


Figure D.2 KC Control 100% Cement Freeze-Thaw Trend



**Figure D.3 Topeka Control 50-50 Freeze-Thaw Trend**



**Figure D.4 KC Control 50-50 Freeze-Thaw Trend**

## Appendix E - Comparison of PCTB with RCA to Control

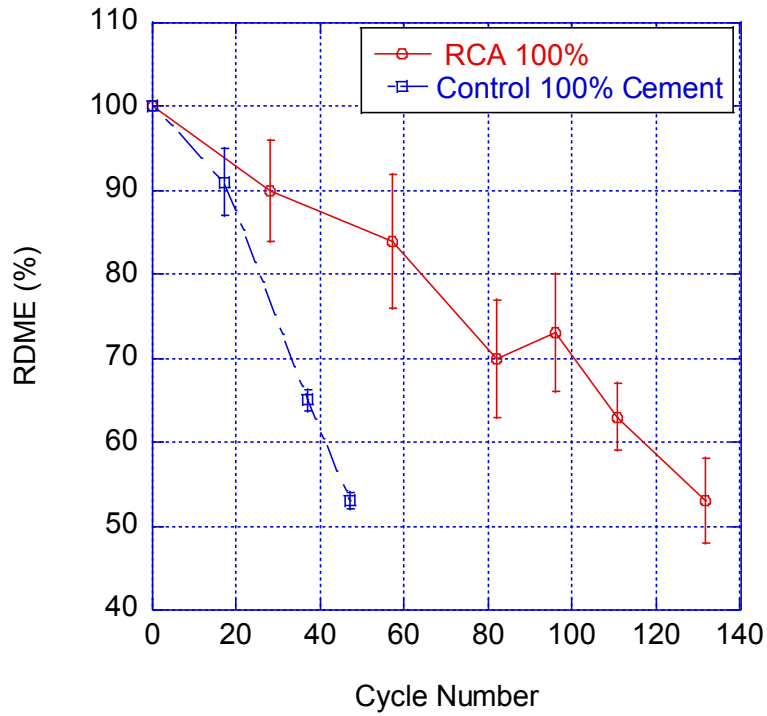


Figure E.1 Topeka 100% Cement Comparison

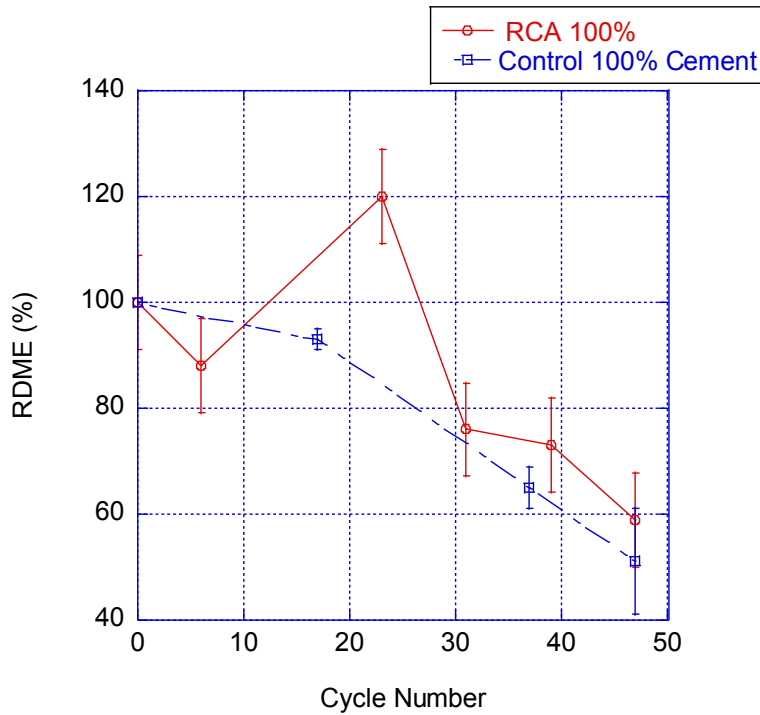


Figure E.2 KC 100% Cement Comparison

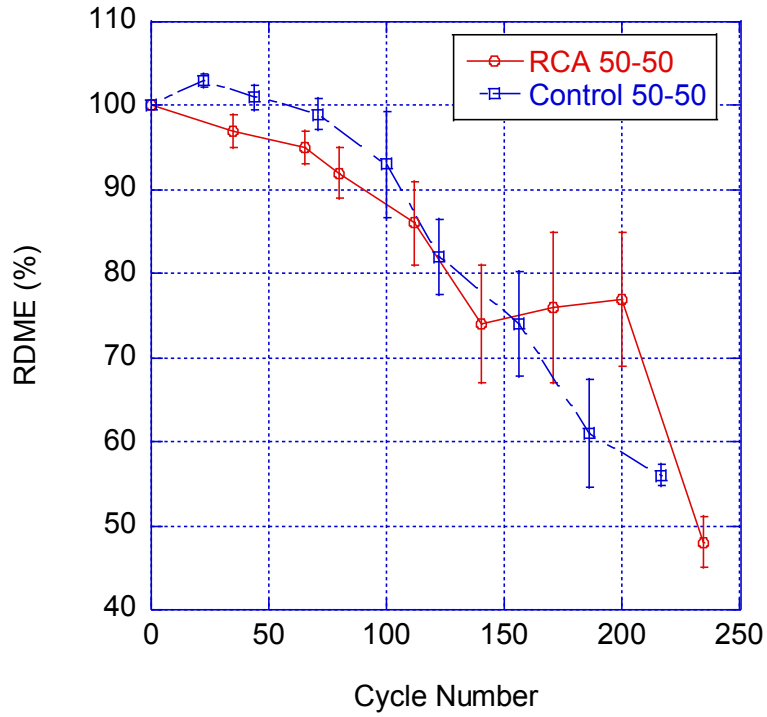


Figure E.3 Topeka 50-50 Comparison

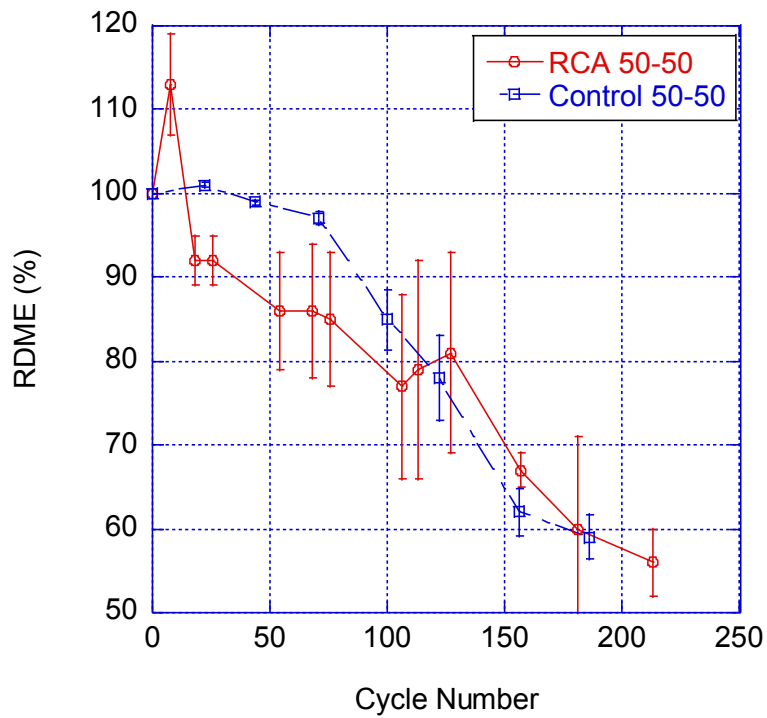
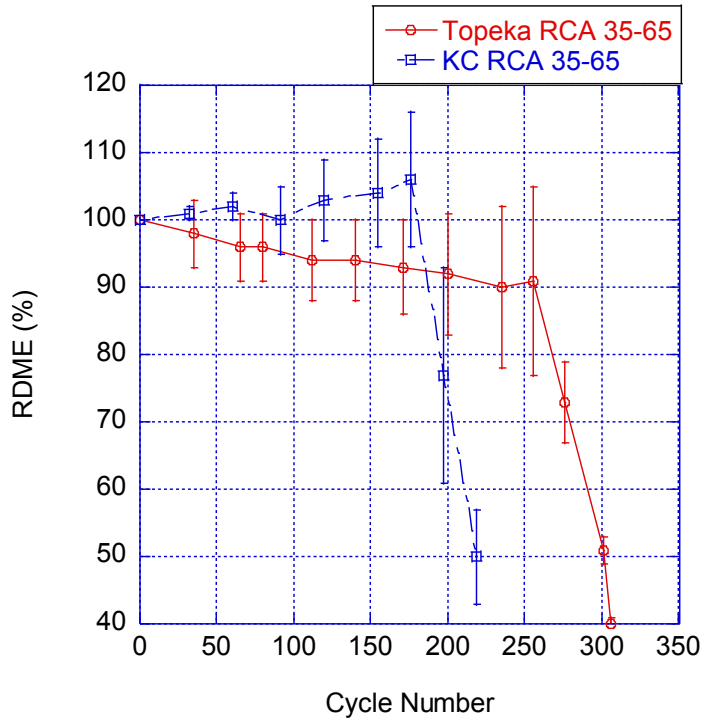


Figure E.4 KC 50-50 Comparison



**Figure E.5 Topeka & KC 35-65 Comparison**